EVOLUTIONARY BIOLOGY

Phylogenomics establishes an Early Miocene reconstruction of reef vertebrate diversity

Chase D. Brownstein[1]*, Richard C. Harrington[2], Laura R. V. Alencar[1], David R. Bellwood[3], John H. Choat[3], Luiz A. Rocha[4], Peter C. Wainwright[5], Jose Tavera[6], Edward D. Burress[7], Martha M. Muñoz[1,8], Peter F. Cowman[3,9], Thomas J. Near[1,8]

Oceans blanket more than two-thirds of Earth's surface, yet marine biodiversity is disproportionately concentrated in coral reefs. Investigating the origins of this exceptional diversity is crucial for predicting how reefs will respond to anthropogenic disturbances. Here, we use a genome-scale dataset to reconstruct the evolutionary history of the wrasses and parrotfishes (*Labridae*), which rank among the most species-rich and ecologically diverse lineages of reef fishes. We show that major labrid clades experienced pulses of evolutionary innovation and accelerated diversification during the Miocene approximately 20 to 15 million years ago that the origin of no single phenotypic trait can explain. These results draw parallels to the evolutionary histories of many clades after mass extinctions and corroborate recent fossil evidence for an Early Miocene extinction event in oceanic vertebrates and changes in coral reef faunal composition. Our data provide genomic evidence for a major Early Miocene reassembly of reef faunas.

INTRODUCTION

Mass extinctions are engines in the generation of biodiversity. These events and the subsequent invasion of newly available ecological niches by survivors are thought to explain the origins of major swaths of extant species (*1*–*6*). There is now strong evidence that the early diversifications of major clades like birds (*7*–*11*), snakes (*12*), frogs (*13*), spiny-rayed fishes (*14*–*17*), and mammals (*18*–*21*) were tied to ecological opportunity created by the mass extinction at the Cretaceous-Paleogene boundary 66 million years (Ma) ago. Yet, extinction and turnover events in the past 60 Ma have dramatically reshuffled biotas and represent near-equally important macroevolutionary events for understanding the formation of living species richness (*22*–*27*). This is particularly apparent for marine biotas; clades as varied as sharks and corals appear to have been far less affected by the Cretaceous-Paleogene mass extinction than their terrestrial contemporaries (*28*–*36*). Instead, the formation of present-day oceanic ecosystems, especially species-rich coral reefs, appears connected to extinctions that have taken place over the past 33 Ma (*33*–*35*, *37*–*42*) and the rise and fall of major oceanic biodiversity hotspots (*39*, *43*–*45*). Pinpointing the timing of these events is difficult because of gaps in the fossil record and limited sampling of living marine biodiversity, as well as conflicting evolutionary timescales estimated for species-rich assemblages like marine fishes (*36*, *43*, *46*–*51*).

Labridae, which includes the iconic wrasses, hogfishes, razor fishes, and parrotfishes, is one of the most species-rich and ecologically diverse living marine fish clades and a major component of global reef vertebrate diversity (*47*, *52*–*54*). Here, we resolve the phylogenetic relationships of the major labrid lineages using a genome-scale dataset and explicitly test how different calibration strategies and models of molecular evolution affect estimates of the timescale of labrid evolution. We robustly infer a major pulse of radiations (Fig. 1) across *Labridae* that unfolded during the Early Miocene, a period of global climate stability (*41*, *55*–*58*). This event generated independent shifts in evolutionary optima for ecologically relevant traits and saw the origination of numerous evolutionary novelties and innovations at the base of each radiation. These temporally concurrent radiations also correspond to a pronounced uptick in labrid dispersal events across oceans, suggesting a global pattern of rapid diversification. Our results reveal the phylogenomic signal of a major reassembly of reef fish diversity approximately 20 Ma ago during a period of global climate stability, an event hinted at by evidence from the invertebrate fossil record (*33*, *39*, *40*, *59*, *60*). The multiple concurrent radiations of different lineages of labrids provide strong support for a global event that restructured oceanic ecosystems during the Early Miocene and shaped their present biota.

RESULTS

The origin and diversification of *Labridae*

We inferred the phylogenetic relationships of *Labridae* from approximately 1000 ultraconserved element (UCE) loci sequenced for 498 specimens comprising 415 of 674 the currently recognized labrid species according to Eschmeyer's Catalog of Fishes (accessed January 2023). Phylogenetic analyses using multiple data partitioning strategies resolved the relationships of the major linages of *Labridae*, including the previously unresolved position of the fairy and flasher wrasse clade *Cirrhilabrinae* (*54*, *61*) as the sister clade to a lineage containing slingjaw and humphead wrasses (*Cheilininae*), tautogs and relatives (*Labrinae*), and parrotfishes (*Scarinae*), with robust node support (bootstrap = 100, coalescent support = 1.0) (Fig. 1A, figs. S1 to S8, and Supplementary Text). *Hypsigenyinae* is placed as the sister lineage of all other wrasses. We also resolve genus-level relationships among the most diverse labrid families, including a sister relationship of tuskfishes (*Choerodon*) and cales and weedwhitings

[1]Department of Ecology and Evolutionary Biology, Yale University, Class of 1954 Environmental Science Center, 21 Sachem Street, New Haven, CT 06511, USA. [2]Department of Natural Resources, Marine Resources Research Institute, 217 Ft. Johnson Road, Charleston, SC 29412, USA. [3]College of Science and Engineering, James Cook University, Townsville, QLD 4811, Australia. [4]Section of Ichthyology, California Academy of Sciences, 55 Music Concourse Drive, Golden Gate Park, San Francisco, CA 94118, USA. [5]Department of Evolution and Ecology, University of California, Davis, Davis, CA 95616, USA. [6]Departamento de Biología, Universidad del Valle, Cali, Colombia. [7]Department of Biological Sciences, University of Alabama, Tuscaloosa, AL 35487, USA. [8]Peabody Museum, Yale University, 21 Sachem Street, New Haven CT 06511, USA. [9]Biodiversity and Geosciences Program, Queensland Museum Tropics, Townsville, QLD 4810, Australia.
*Corresponding author. Email: chase.brownstein@yale.edu

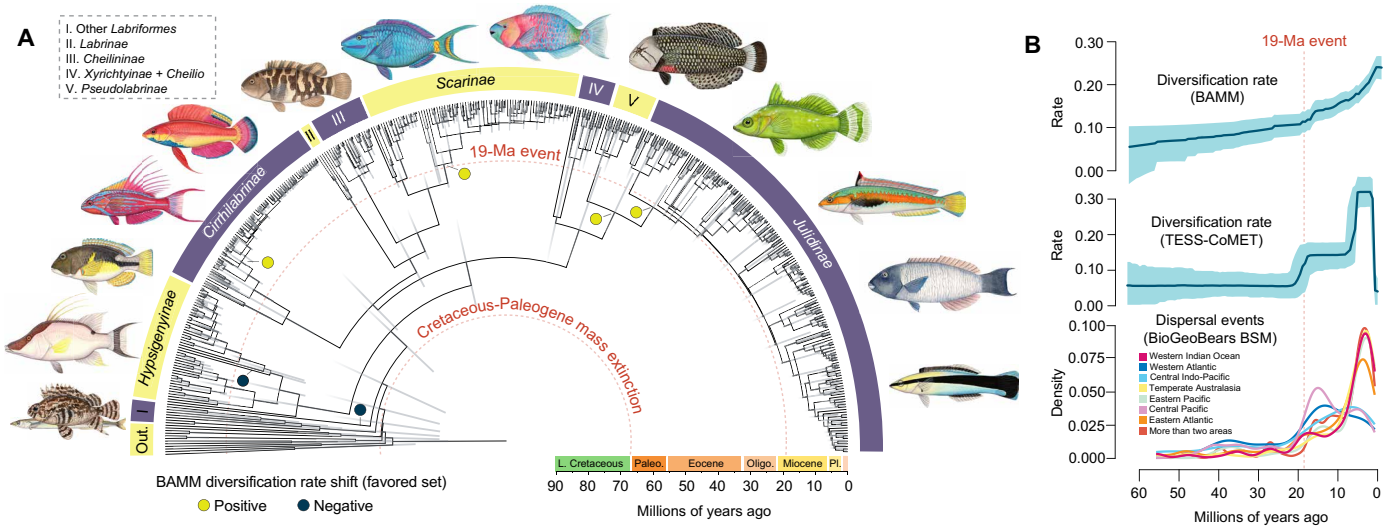

Fig. 1. Explosive Early Miocene radiations occurred in multiple clades of labrid fishes. (**A**) Node-dated phylogeny of *Labridae* using inferred three sets of 50 UCEs randomly chosen from the set of 1009 sequences, the GTR substitution model, and the ASTRAL-III species tree topology. Bars at nodes indicate 95% highest posterior density intervals for divergence times. (**B**) Different metrics of diversification and biogeographic change through time. The dispersal plot (lowest) shows the density of dispersal events to particular areas, where dispersals are divergence events following the movement of individuals in an ancestral population to a new region followed by speciation from the ancestral population. Illustrations by J. Johnson (https://lifesciencestudios.com/).

traditionally placed in the family "*Odacidae*" (*Odax*, *Olisthops*, *Neoodax*, and *Haletta*), placement of the tuskfish genera *Clepticus* and *Semicossyphus* within the genus *Bodianus*, reciprocal monophyly of coral and seagrass-bed–associated parrotfishes, and polyphyly of the species-rich julidine genera *Coris* and *Halichoeres*, as in previous studies (*16*, *54*, *61*–*63*).

Using the UCE data and a set of 13 fossil calibrations (fig. S9), we time calibrated the phylogeny of *Labridae*. We used several models of nucleotide evolution [e.g., general time reversible (GTR) and Hasegawa-Kishino-Yano (HKY)] and applied both node-dating and tip-dating approaches to produce multiple time-calibrated phylogenies and test the influence of different prior specifications on our inferences of divergence times. Justifications for the placement of fossil calibrations are in the Supplementary Materials. The inferred timetrees all support a post-Cretaceous origin of the *Labridae* and Eocene divergence among its major subclades (Fig. 1, figs. S9 to S12, and Supplementary Text), contrasting with several previous studies that estimated a Mesozoic age for this lineage (fig. S10) (*53*, *54*).

Our time-calibrated phylogeny shows that a set of explosive diversifications took place across *Labridae* starting approximately 19 Ma ago in the Early Miocene (Fig. 1, A and B, and figs. S13 to S16). In total, more than 10 major lineages of labrids, including *Choerodon* and *Bodianus* hogfishes, two lineages of fairy and flasher wrasses in *Cirrhilabrinae*, the *Labrinae*, two major lineages of parrotfishes in the *Scarinae*, the *Xyrichtyinae,* and the *Julidinae* and several of its most species-rich subclades, radiated independently during the Early Miocene (Fig. 1).

Historical biogeographic reconstruction indicates that this event corresponds to an increase in dispersal events, as reconstructed on the time-calibrated phylogeny of *Labridae* (Fig. 1B). Increases in lineage accumulation and diversification rates are detected in different analyses of node-dated phylogenies made using different models of sequence evolution (figs. S13 to S16 and Supplementary Text). TESS-CoMET detects an increase in speciation rate during this interval that is supported by Bayes factors of 5 to 6 across analytical iterations using different prior shift counts (fig. S14). Diversification rate curves estimated across time-calibrated phylogenies (Fig. 1B, figs. S13 and S14, and Supplementary Text) and stochastic mapping of dispersal events through time (Fig. 1B, figs. S13 and S17 to S19, and Supplementary Text) suggest that *Labridae* includes multiple evolutionary radiations (rapidly diversifying lineages) that appeared during the Early Miocene. Analysis of lineage diversification using BAMM (fig. S17) suggests that radiations of *Cirrhilabrus* and *Paracheilinus* fairy and flasher wrasses (*Cirrhilabrinae*) and *Scarus* and *Chlorurus* parrotfishes (*Scarinae*; Fig. 1A) are among the most rapidly diversifying lineages of vertebrates (*64*, *65*). The Early Miocene burst of labrid diversification is especially stark in the clade *Julidinae*. Within julidines, at least eight globally distributed lineages comprising hundreds of species diverged in less than 3 Ma (Fig. 1A and figs. S11, S12, and S15). Our inferences of the historical biogeography and diversification of *Labridae* remain comparable across time-calibrated phylogenies generated using different models of nucleotide evolution (fig. S13) and when input priors for these analyses (e.g., TESS-CoMET) are varied (fig. S14). Together, these results identify the Early Miocene as a major period of diversification in wrasses and parrotfishes.

Dynamics of the largest reef fish radiation

To investigate whether the explosive diversification of labrid lineages in the Early Miocene are associated with the evolution of ecologically and functionally relevant traits, we reconstructed the evolution of 10 discrete and 12 continuous characters related to the myology and skeletal anatomy of the skull and fins, body size, and dietary niche using the time-calibrated phylogenomic tree of the *Labridae* (Fig. 1A). Many of these traits are putative key innovations in the *Labridae* that may have facilitated the invasion of new ecologies and subsequent rapid speciation (*47*, *52*, *53*, *62*, *66*–*69*). Ancestral state reconstructions and state-dependent diversification rates estimates

for the discrete cranial characters demonstrate that many evolutionary novelties, including the "parrotfish pharyngeal jaw" condition, the intramandibular joint, and a transition to bite-based feeding from suction feeding, originated in several lineages concurrently during or just following the Early Miocene diversification event (Fig. 2, A and B). Yet, the diversification rates associated with clades having these traits do not significantly differ from those of other labrids. Comparisons between binary state speciation and extinction (BiSSE) and hidden state speciation and extinction (HiSSE) models favored character-independent hidden state models for all traits except two of the three combinations of the biting/suction character state analyzed (Table 1 and Supplementary Text); the character-dependent HiSSE models favored for the two permutations of the biting/suction trait do not show a clear effect of either trait on diversification rates. These suggest that diversification across labrid fishes is not explained by innovations exclusive to only one or a few labrid lineages.

We obtained similar results from reconstructing changes in the disparity of continuous characters through time. We found that *Labridae* experienced a period of high within-clade disparification falling outside 95% confidence intervals for Brownian motion in most continuous characters, including body mass, standard length, jaw protrusion, and jaw muscle size (*M. adductor mandibulae* and *M. levator posterior* masses), starting at 19 to 20 Ma ago (fig. S20). Model fitting suggests that an Orstein-Uhlenbeck (OU) model best fits the pattern of evolution of the continuous characters examined (table S1 and Supplementary Text). This allows us to reject the hypothesis that the disparification of ecologically relevant cranial and fin characters followed an early-burst pattern as expected if a single adaptive radiation originated at the most recent common ancestor (MRCA) of *Labridae*. A principal components analysis of the continuous characters related to cranial morphology and body size in *Labridae* demonstrates that morphospace expansion was achieved in clades that radiated in the past 10 Ma (fig. S21). The parrotfish lineages *Scarus* and *Chlorurus* occupy a unique region of morphospace, highlighting the innovative nature of their cranial morphology (*53*, *68*).

We identified the locations of adaptive shifts in continuous character values along the phylogeny of the *Labridae* using the R package bayou, which fits a multi-peak OU model to detect adaptive shifts in trait optima (θ) through time (*70*). Our results show that 77.2% (34 of 44) of detected optima shifts occurred following the start of the Early Miocene event. The number of θ shifts that we detect peaks at approximately 6 to 11 Ma ago after starting to increase in the Early Miocene (Fig. 3B). Shifts in θ were concentrated in the lineages *Cirrhilabrinae*, *Scarinae*, and *Julidinae* (Fig. 3A), which are the three clades that show the most pronounced increases in diversification rates during the Early Miocene (Fig. 1, A and B, and figs. S15 and S16). Specifically, the θ shifts in the parrotfishes mainly corresponded to changes in body size, whereas in *Cirrhilabrinae* and *Julidinae*, the shifts primarily involved functional characteristics of the jaws and fins (Fig. 3A and Supplementary Text). These results indicate that potentially adaptive shifts in functionally relevant anatomical traits occurred simultaneously and independently in multiple wrasse lineages that underwent explosive diversification in the Early Miocene (Fig. 1).

Together with our trait-associated diversification rate estimates, our reconstruction of the disparification of functionally relevant traits through time (Fig. 3) supports the differential adaptive evolution of functionally relevant characters of the skull and fin in individual

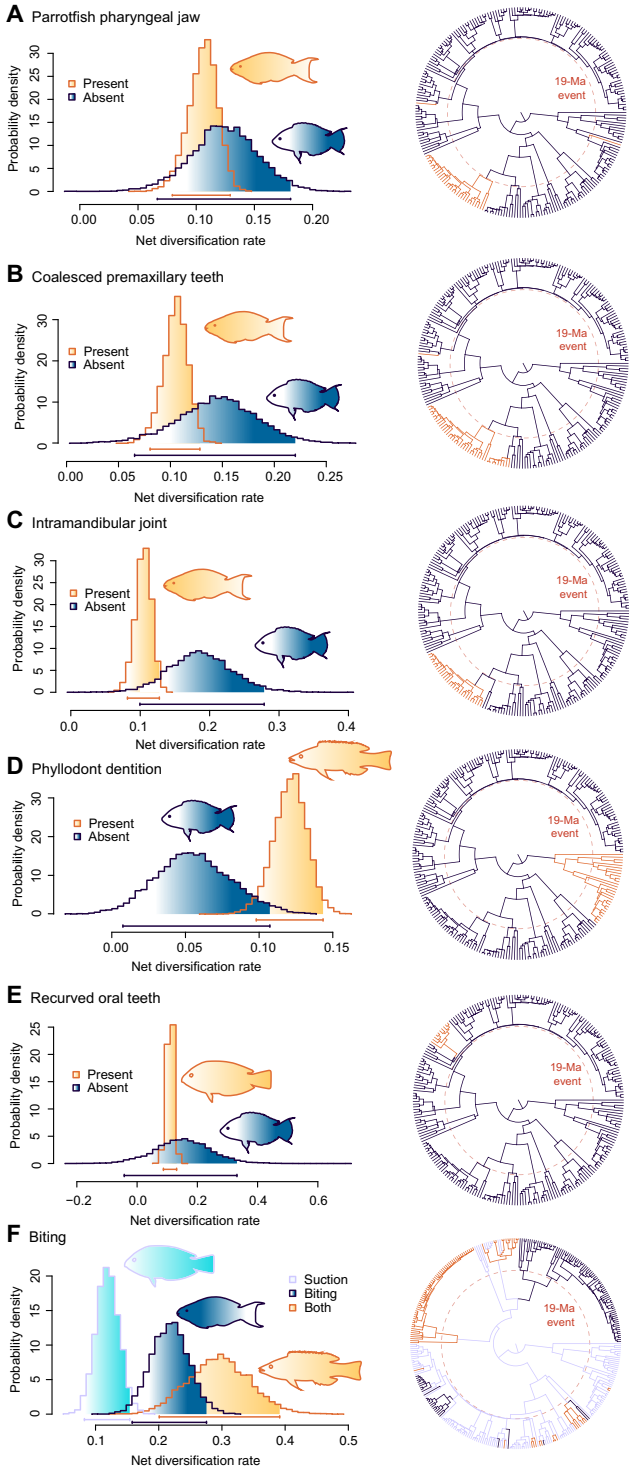

Fig. 2. Evolutionary history of labrid key innovations suggests that no one feature clearly explains the living diversity of wrasses, parrotfishes, and relatives. (**A** to **F**) show the trait-associated diversification rates estimated using BiSSE and MuSSE (left) and simulated stochastic mapping–based ancestral state reconstructions along the timetree of *Labridae* (right) for six functionally important craniodental characteristics that are considered to be key innovations in *Labridae*.

Table 1. Comparison of trait-based diversification rates across labrid discrete traits shows that HiSSE models are weakly favored, but, in most cases, hidden-character–independent models are more favored than hidden-character–dependent models. Table shows corrected Akaike information criterion (AIC) scores calculated for four models of trait-based diversification, with the AICc score associated with the best-fit model bolded. HiSSE CD, character-dependent HiSSE model; HiSSE CID, character-independent HiSSE model.

Discrete trait	Null model	BiSSE	HiSSE CD	HiSSE CID
Coalesced premaxillary teeth	1518.22058	1513.331677	1489.361736	1483.898186
Intramandibular joint	1503.11	1491.894	1471.226	1468.789
Phyllodont dentition	1490.717115	1485.367755	1467.801438	1456.395399
Parrotfish pharyngeal jaw	1509.116851	1520.018725	1477.848313	1474.796238
Recurved oral teeth	1493.595616	1493.614258	1470.082867	1459.273276
Biting only versus other	1948.458188	1942.789017	1905.061756	1897.940665
Biting and suction versus other	2020.592988	2006.43114	1948.227028	1970.075464
Suction only versus other	1983.909671	1979.321184	1839.511741	1927.636208
Reef association	2472.817752	2414.024582	2252.066888	2408.485385

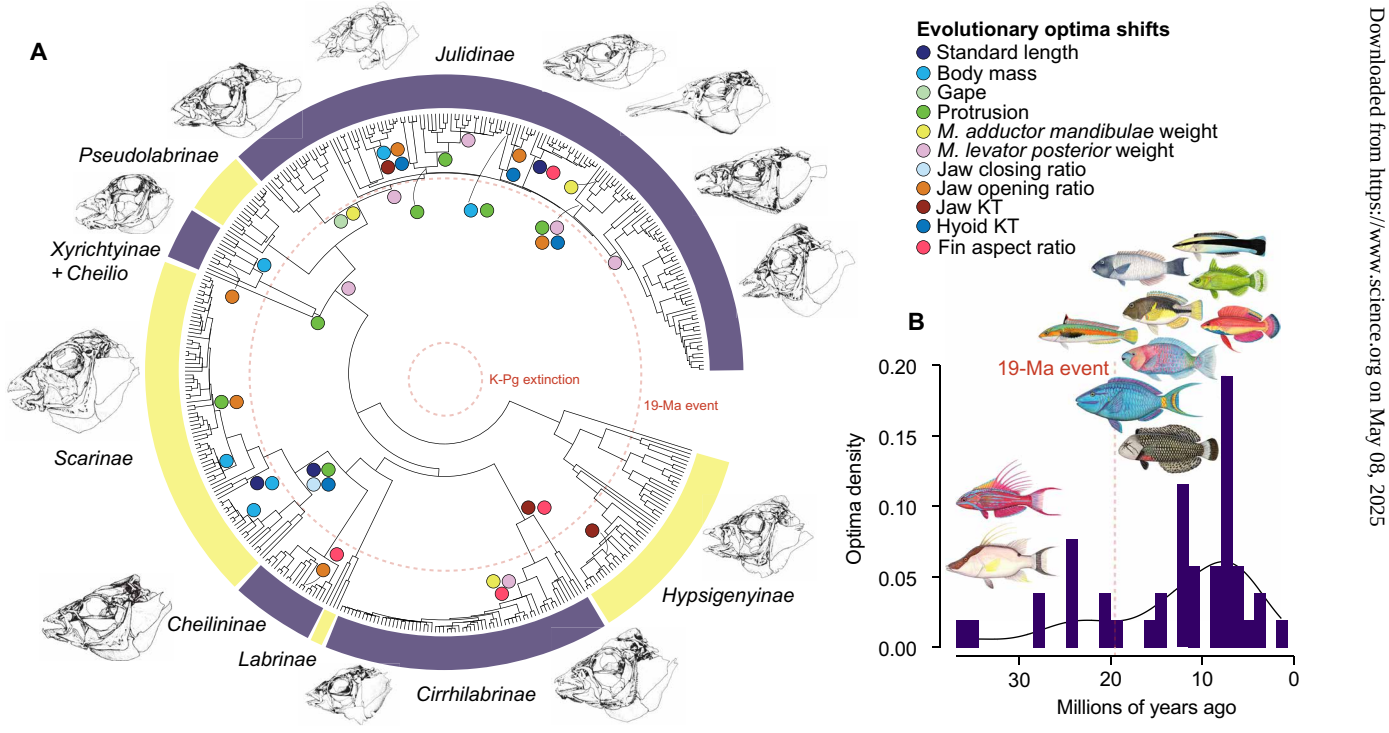

Fig. 3. Timescale and location of optima shifts for key labrid features supports the Early Miocene as a time of morphological innovation. Time-calibrated phylogeny of labrid fishes in (**A**) is annotated to show the position of trait optima shifts for 11 functionally and ecologically important continuous traits in *Labridae*. Of the 12 traits examined, all showed shifts except for the *M. sternohyoides* mass. Histogram in (**B**) shows the density of optima over the evolutionary history of *Labridae*. Note that no optima occur before 40 Ma, and a marked increase occurs after 20 Ma continuing to just after 10 Ma. Illustrations by J. Johnson (https://lifesciencestudios.com/).

labrid clades. The evolution of functionally important labrid cranial and postcranial features mainly relates to the evolution of lineage-specific features. On a larger scale, the absence of a detected diversification rate shift associated with the common ancestor of *Labridae* and *Centrogenys* suggests an indirect relationship between the acquisition of the labroid pharyngeal jaw in this clade and its species diversity (*47*, *71*–*73*). Together, these results suggest that no single key innovation in cranial anatomy or function alone explains the diversity observed in the *Labridae* (Fig. 2) (*74*) and substantiates the present-day diversity of this clade as an assemblage of multiple concurrent evolutionary radiations following an event that initiated in the Early Miocene 19 to 20 Ma ago.

The Early Miocene and the origin of living reef biotas

What instigated the concurrent radiations of labrid fishes during the Early Miocene? Multiple paleoclimate proxies indicate that global

climate at 19 to 20 Ma was relatively stable (*41*, *56*, *58*, *75*) in contrast to the pattern that might be expected to cause major extinction or biotic turnovers. However, recent evidence points to turnover events across oceanic ecosystems during this time, despite the climatically unremarkable conditions. For example, the generic diversity of corals in the Caribbean and Mediterranean decreased by 30 to 50% (*59*, *60*). Although the diversification of the major reef-building coral clade *Scleractinia* occurred in the past 5 Ma, the fossil record suggests that this lineage began to dominate reef coral assemblages at approximately 20 Ma (*76*). Recent studies suggest that this period also marked an increase in associations between reef fishes and living corals (*40*). The Early Miocene featured the migration of the major reef biodiversity hotspot to its present location in the Indo-Pacific (*44*, *45*, *77*–*80*), which holds a sizeable proportion of present-day species diversity of the *Labridae* (*39*, *81*). Our results suggest that post-Miocene rapid diversification events in labrid fishes (Fig. 1A and figs. S15 and S16) involve lineages with centers of diversity in the Indo-Pacific Biodiversity Hotspot, such as *Cirrhilabrus* fairy wrasses and *Scarus* and *Chlorurus* parrotfishes (*44*, *82*, *83*). We also infer a Plio-Pleistocene diversification of the parrotfish genus *Sparisoma* in the western Atlantic Ocean (figs. S11 and S15). Together, these recent, secondary diversification events account for increased overall rates of diversification from the Early Miocene to recent. Thus, our results indicate that despite the stable global climate of the Early Miocene, this period featured the initiation of explosive, concurrent radiations observed within labrid fishes that were enabled by extinction and turnover across marine ecosystems.

Our analyses pull the estimated ages of the labrid radiations toward the present by 10 Ma compared to earlier estimates (fig. S3). Previous studies based on smaller, legacy marker datasets and more limited species sampling suggested the Miocene was important in the evolution of wrasses and other lineages of reef fishes (*44*, *62*). However, our results support a set of younger and far more explosive diversifications in labrids that initiated during the Early Miocene compared to other analyses (*44*, *62*, *68*, *84*, *85*). There is preliminary evidence that this discrepancy affects other reef fish clades. For example, a recently published timetree of butterflyfishes (*Chaetodontidae*) (*43*) estimated Middle Miocene ages for genera that postdate previous estimates made using legacy nuclear and mitochondrial genes (*49*, *65*) by 5 to 10 Ma. This result is consistent with previous studies that demonstrate mitochondrial gene sequences, which are prone to saturation, yield far older divergence times in relaxed molecular clock analyses (*86*).

To investigate whether reef association or trophic evolution are linked to the Early Miocene radiations of wrasse lineages, we conducted ancestral state reconstructions of dietary mode and coral reef association on the time-calibrated phylogeny (Fig. 4). These reconstructions of dietary mode suggest that labrids ancestrally preyed on shelled invertebrates before exploiting a variety of different food items starting at 19 to 20 Ma (Fig. 4A). The phylogenetic ancestral state reconstructions record at least seven major shifts in dietary ecology from an ancestral shelled invertebrate diet toward specialized feeding in the Early Miocene, including in a temperate Australian clade of *Hypsigenyinae*, *Cirrhilabrinae* (excluding *Pteragogus*), *Labrinae*, *Cheilininae*, one or two clades in *Scarinae*, and four subclades in *Julidinae* (Fig. 4A). In addition, all cleaner-wrasse clades originated and diversified within the past 11 Ma (Fig. 4A and fig. S21), implying a rapid acquisition of the cleaning ecomorphology (*63*). The evolution of cleaning behavior in these clades is complex, with multiple origins of facultative and obligate cleaners (Fig. 4B). Our inference that numerous labrid clades experienced rapid diversification and phenotypic innovation along with concurrent major shifts in dietary ecology strongly supports their status as radiations (*2*, *5*, *6*).

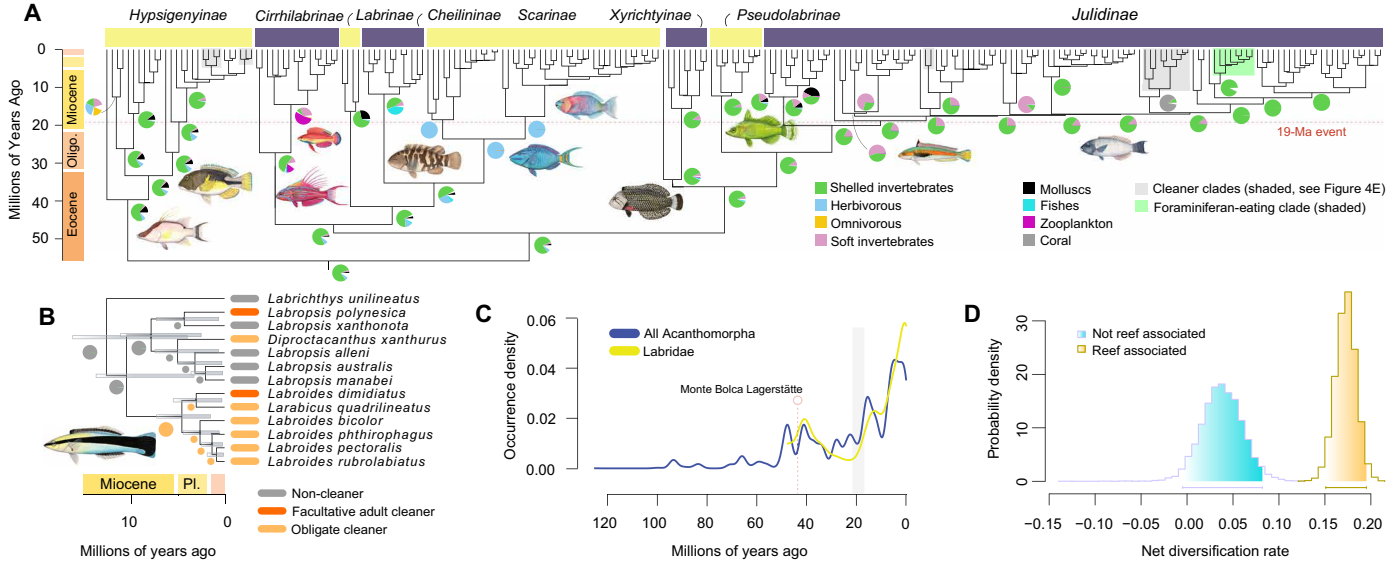

Fig. 4. Trophic shifts and reef association drove the independent explosive radiations of labrid fishes at 20 Ma. Time-calibrated phylogeny of labrid fishes in (**A**) is annotated with an ancestral state reconstruction of diet across labrid fishes (for each pie chart, only the top four most probable states are shown). Phylogeny in (**B**) shows the complex evolution of one novel ecology-cleaning in the most diverse single clade of cleaner wrasses. Note that obligate and facultative adult cleaners each evolve twice according to this ancestral state reconstruction. (**C**) shows fossil occurrence density curves for *Labridae* and *Acanthomorpha*. (**D**) shows the trait-associated diversification rates for the reef association trait as found in BiSSE. Note the marked, continuous increase in labrid fossil occurrences after 20 Ma that is consistent with the results in this study but differs from the timescale of labrid evolution inferred in previous analyses (fig. S3). Illustrations by J. Johnson (https://lifesciencestudios.com/).

The rapid radiations and trophic expansions of these labrid subclades mirror the labrid fossil record, which shows an increase in labrid occurrences exceeding the background fossil record of *Acanthomorpha* from the Early Miocene to the Quaternary (Fig. 4C and Supplementary Text). Together, these findings indicate that the Early Miocene saw rapid diversification of labrid lineages into a variety of novel dietary niches that coincided with the expansion of coral reef ecosystems (*87*) and the formation of the Indo-Pacific Biodiversity Hotspot in its present location (*45*, *77*, *79*). These ecological innovations included the emergence of the cleaning ecomorph from a lineage of coral mucus feeders and the origin of feeding on foraminifera (Fig. 4A).

We infer that the MRCAs of *Labridae* and nearly all labrid subclades were reef-associated (fig. S10A), in contrast to some previous reconstructions (*68*). Furthermore, trait-based diversification rate analyses strongly support the hypothesis that the use of reef habitats has a stronger association with the diversification of labrid fishes (Fig. 4D) compared to any other examined trait (Figs. 2 and 3). Although a character-dependent HiSSE model is the best fit for the reef-association trait, examination of the underlying hidden states and their associated rate values shows that most labrids not associated with reefs are assigned to a hidden state (a) with low rate values, while reef-associated labrids are distributed across either hidden state (a or b), both of which exhibit much higher rates than almost all nonassociated species (fig. S22 and Supplementary Text). These results suggest that the global concurrent radiations of labrid subclades in the Early Miocene were driven by major ecological changes to oceans, including the reassembly of coral diversity and structure of reefs (*40*). Together, these results highlight the importance of trophic shifts and increased reef association in explaining the present-day diversity of *Labridae* (*46*, *84*). The radiation of multiple lineages of *Labridae* during the Early Miocene appears to have been facilitated by intimate ecological ties to the restructuring coral reef ecosystems of that time period.

DISCUSSION

The results of our comparative analyses using the time-calibrated phylogenomic tree present a revised scenario for the origins of the exceptional biodiversity observed in the *Labridae*. First, we resolve the relationships of all major labrid clades, including the placement of hogfishes, cales, and tuskfishes (*Hypsigenyinae*) as the living sister clade to all other labrids and the fairy wrasses (*Cirrhilabrinae*) as the sister clade to a lineage containing tautogs and relatives (*Labrinae*), slingjaw and humphead wrasses (*Cheilininae*), and parrotfishes (*Scarinae*) (*54*, *61*–*63*). Our resolution of the major labrid clades and species-level phylogenetic relationships within them allows us to investigate the tempo of labrid diversification, the origination of key innovations, and the evolution of novel ecologies at high level of detail.

Instead of accumulating through protracted lineage diversification over the past 50 Ma (*44*, *52*), we locate the origins of living labrid diversity within iterative bouts of radiations that took place during the Early Miocene and which fueled accelerated diversification to the present (Fig. 1). Our analyses suggest that these radiations were tied to global changes in reef-building coral diversity and structure and eliminate major climate shifts (Fig. 1A and fig. S2) (*54*) or the origination of individual key innovations (Fig. 2) (*47*, *53*, *74*) as the primary drivers of species richness across labrid phylogeny. Although labrids have displayed notable morphological diversity over the past 50 Ma (*88*–*91*), the key innovations of living labrid clades are much younger, originating over an approximately 5-Ma period in the Early Miocene (Figs. 2 and 3).

By tracing the biogeography of labrids through time, our results also support an Early Miocene age for key reef biodiversity centers such as the Indo-Pacific Biodiversity Hotspot (*33*, *44*, *45*, *83*), which we infer as the ancestral region for the major labrid clades *Cirrhilabrus*, *Cheilininae*, *Choerodon*, *Julidinae*, and *Pseudolabrinae* (Fig. 1 and figs. S11 and S12). The Early Miocene ages of these labrid radiations are comparable to bursts of diversification observed in several clades of animals that correspond to the assembly of the present-day marine biodiversity hotspot in the Indo-Pacific (*79*). This suggests a broad signature of reef faunal turnover and ecological restructuring during the Early Miocene that is decoupled from any known mass extinction or rapid climate change event. Instead, this pulse of diversification corresponds to major ecological restructuring tied to hotspot relocation and formation.

The timescale of labrid diversification and associated phenotypic innovation that we reconstruct provides insight into the synergistic influences of habitat preference, trophic specialization, and novel morphologies on the species richness of different labrid clades (*53*, *68*, *74*). Labrids concurrently evolved morphological innovations (Figs. 2 and 3) and used novel dietary resources (Fig. 4) as they explosively radiated during the Early Miocene. Rather than being secondarily occupied by wrasses, reefs may have directly facilitated concurrent radiations in *Labridae*. This scenario highlights the potential role that Early Miocene changes to reef biota composition and the physical structure of reefs themselves (*59*, *60*, *76*) may have had in driving fluctuations in labrid diversity through time. If reefs were the ancestral habitat for labrid fishes, changes to reef habitat availability and location that occurred during this time (*45*, *77*, *78*, *92*) would have directly affected their ecology, explaining the reconstructed shifts in lineage diversification rates in the Early Miocene without requiring major shifts in habitat preference. Consequently, the evolutionary history of labrid fishes demonstrates how changes to ecosystem composition in the past 20 Ma drastically affected marine diversity, a critical consideration as fragile reef ecosystems face growing anthropogenic threats.

MATERIALS AND METHODS

Phylogenetic nomenclature

In this study, we use rank-free phylogenetic nomenclature (*93*, *94*) with the names of ray-finned fish clades following a recent phylogeny-based classification (*95*). We note that our study demonstrates that several genera of *Labridae* are not monophyletic and require extensive taxonomic revision, but, at this time, we refrain from proposing changes to the generic classification of labrids. Following emerging trends in phylogenetic nomenclature (*94*–*97*), including a recent wholesale revision of the systematics of ray-finned fishes in accordance with phylogenetic taxonomic principles (*95*), we italicize all formal taxonomic names.

Taxon sampling and sequencing

Labridae is one of the most species-rich lineages of acanthomorph, or spiny-rayed, fishes, comprising 674 valid and recognized species classified in 76 genera (*98*). Previous analyses of the phylogenetic relationships of labrid fishes show that several species-rich genera, particularly those in the *Julidinae*, are likely paraphyletic (*54*, *61*–*63*). To produce a rigorous hypothesis of the phylogeny of *Labridae*, we

sampled 498 individuals including at least 398 species (as well as 17 undescribed forms) and 70 genera, representing 92% of the genera, 59.1% of species, and all of the recognized subfamilies of *Labridae*; our taxon sampling includes the phylogenetic diversity required for comparative analyses this clade. We combined novel UCE sequence data from 424 (one, *Achoerodus viridis*, was sequenced twice) individuals with UCE sequences from 47 species of cirrhilabrine wrasses included in a phylogenomic analysis of *Cirrhilabrus* (*83*) and UCE sequences from 26 individuals in *Hypsigenyinae*, *Julidinae*, *Labrinae*, *Cheilininae*, and *Scarinae* taken from a phylogenomic analysis of *Acanthomorpha* (*16*)]. We also sampled 20 species from other lineages of *Eupercaria* as outgroups. We constructed alignments of 1009 UCE loci that were sequenced from a bait set of 1341 UCE loci designed for acanthomorph fishes using DNA extraction, library construction, and sequencing protocols modified from earlier studies (*16*, *17*, *97*, *99*). Newly generated DNA sequence were pooled with those from earlier phylogenetic studies of acanthomorphs (*16*, *83*). Tissue samples were preserved in 80 to 100% ethanol and stored at −20°C before extraction using a DNeasy Blood and Tissue kit (Qiagen, Hildren, Germany). Library preparation, enrichment, and sequencing were performed by Arbor Biosciences (Ann Arbor, MI, USA) following methods described by Cowman *et al.* (*100*). Following target-capture enrichment, target-enriched libraries were sequenced on one lane of Illumina HiSeq 2500 (100–base pair paired-end reads). Our dataset represents a substantial expansion on previous datasets that deployed selected Sanger-sequenced nuclear and mitochondrial genes (*61*, *62*) and phylogenomic exon datasets (*54*) to infer the phylogenetic relationships of *Labridae*. Recent work has also shown that large UCE datasets might preserve higher levels of phylogenetic signal than other genome-scale DNA sequence data, including exons (*101*, *102*).

Assembly and preprocessing of molecular data

UCE alignments were processed, assembled de novo, and checked for paralogs using the bioinformatics pipeline phyluce 1.7.1 (*103*) on the James Cook University High Performance Computing Cluster. The assembly step was performed outside of phyluce using Spades v. 3.10 (*104*, *105*) with the "–careful" and "–cov-cutoff 2" parameters. After the UCE loci were extracted from assembled contigs and aligned, a 75% matrix was created for phylogenetic reconstruction. Using an initial batch of gene trees generated using the maximum likelihood phylogenetic analysis software IQ-TREE v. 2.2.0 (*106*), we further sanitized our data by using TreeShrink (*107*) to identify and remove trees from the gene tree set with abnormally long branches. As a further sanitization check, we personally examined every UCE alignment by eye to identify chimeric sequence data, which may affect many UCE datasets (*97*). Following these steps, the phylogenomic dataset consisted of 1009 UCE loci.

Maximum likelihood phylogenetic analysis and assessment of node support

We conducted maximum likelihood phylogenetic analyses using the software IQ-TREE v. 2.2.0 (*106*) on the Yale High Performance Computing Cluster McCleary using three different methods. We analyzed the concatenated UCE dataset under both one partition and under a best-fit scheme selected by PartitionFinder2 (*108*). We inferred gene trees from each individual UCE locus and summarized gene trees using the multispecies coalescent model implemented in ASTRAL III v. 5.7.8 (*109*). For each locus, we identified optimal models of nucleotide evolution using ModelFinderPlus (*110*) and used 1000 ultrafast bootstraps to assess support for nodes resolved in trees produced using IQ-TREE. In addition to the conventional bootstrapping approach for assessing topological support, we calculated gene and site concordance factors using IQ-TREE 2 (*111*). Concordance factors provide an additional measure of support for the inferred phylogeny through assessing the number of gene trees and sites consistent with an input species tree topology (*111*). We calculated site concordance factors using 100 subsampled quartets from the concatenated UCE alignment and then exported the data to R for additional comparisons, including linear regression of gene and site concordance factors, log-transformed branch lengths, and primary and secondary gene and site discordance factors, which measure the number of gene trees and sites that support the most commonly found alternative topology to the species tree topology. Of particular interest upon initial observation of scatterplots contrasting different measures of topological support was the weak relationship between site and gene discordance factors. We ran linear models testing this for both primary and secondary gene and site discordance factors. On the basis of summary statistics, site discordance factors predict gene discordance factors significantly, although r-squared values are low (<0.1) and show violations of linear model assumptions. These low correlation values appear to be driven by a handful of branches with anomalously high gene discordance values (fig. S8), suggesting that a handful of gene trees with strongly supported topologies that differ from the species tree are producing discordance. To get an estimate for how many gene trees are generating this anomalous signal, we counted how many branches have primary gene discordance factors that fall outside the 95% confidence intervals for a regression of primary gene and site discordance factor values.

Bayesian node and tip dating analyses

We used both node and tip-based dating methods to time calibrate the phylogeny of *Labridae* using a vetted set of 13 node and 15 tip calibrations (Supplementary Materials). Fossil calibration placement justification was based on an extensive review of the literature and the identification of multiple informative synapomorphies of inclusive clades (see Supplementary Materials). In the case of one fossil, †*Coris sigismundi*, we could not reliably constrain its position beyond *Julidinae*, so we used it as a calibration for the crown julidine MRCA in the node-dating analysis and treated it as unconstrained within crown *Julidinae* in the tip-dating analyses. We ran all time calibration analyses under a Bayesian framework implemented in BEAST 2.6.6 (*112*, *113*). In both cases, we randomly subsampled three sets of 50 UCE alignments from our dataset and ran iterations using different models of molecular sequence evolution (GTR and HKY) to check for the robustness of our age estimates to model specification. We ran all analyses under a relaxed log-normal molecular clock model and the fossilized birth-death (FBD) model of divergence time estimation as implemented in BEAST 2 (*114*, *115*). Because tip-dating is computationally intensive relative to node dating in BEAST 2, we subsampled 62 labrids representing all major clades for input UCE sequences. For the FBD model, we set rho to 0.6 in the node-dating analyses and to 0.11 in the tip-dating analyses, which are the proportions of living species cataloged in Eschmeyer's Catalog of Fishes included in each dataset. For all analyses, we set the origin before 83.6 Ma. This is the age of the crown syngnathiform †*Gasterorhamphosus zuppichinii*, which is the oldest known definite crown member of the clade containing all percomorphs besides *Gobiiformes*, *Batrachoididae*, and *Ophidiiformes* (*16*, *116*,

117). The upper origin prior bound was set to 145.0 Ma (the Jurassic-Cretaceous boundary and the approximate consensus of the age of crown *Acanthomorpha* found in previous studies) (*14*, *16*, *17*, *118*, *119*), and the lower bound was set to 56.0 Ma [the age of the oldest fossil acanthomorphs, including †*Moyclaybalistes* (*120*), assignable to *Acanthuriformes* (*16*, *95*)]. A wide range for the origin prior was used because the Mesozoic fossil record of the major acanthomorph crown clades suffers from major sampling gaps. We set the diversification rate before 0.05, which is the approximate background rate of diversification in Acanthomorpha found in a prior study using UCEs (*16*). The positions of fossil calibrations were constrained using MRCA priors in all runs. In the node-dating runs, the calibrated nodes were placed under lognormal priors with 97.5% of the probability of the age of the node falling before the inputted age of the fossil calibration. Each of the three sets of UCE alignments were analyzed in BEAST three times independently, each for 200 million generations with a 100 million generation pre-burn-in. We checked for convergence of the posteriors and sufficient ESS values using Tracer v 1.7 (*121*) with a 50 million generation burn-in for the tip-dated runs and 75 million generation burn-in for the node-dated runs, and combined posterior tree sets in LogCombiner 2.6.6, with a 75% burn-in and sampling every 10,000 generations for each node-dated posterior tree set and a 50% burn-in and sampling all generations for each tip-dated posterior tree set. Last, we annotated a target tree based on the ASTRAL-III species tree topology using the resulting pooled posterior tree sets in TreeAnnotator using common ancestor heights for the node-dated trees and created maximum clade credibility trees from the tip-dated posterior trees with median node heights.

Comparison of time calibrated phylogenies

Several studies have demonstrated that the methodological choices and model specifications used can significantly affect the estimation of time-calibrated phylogenies within a Bayesian framework (*122*–*124*). To rigorously infer the diversification of *Labridae* through time, we explored the posterior tree sets generated from the analyses in BEAST using various methods. We compared the time-calibrated phylogenies obtained using both tip-dating and node-dating approaches. We did this by directly comparing the 95% highest posterior density intervals of key divergences in the history of labrid diversification, as well as by comparing the shape of lineage-through-time plots generated for each tree using the R packages ape (*125*) and phytools (*126*).

Comparative diversification rate estimates

We used multiple methods to estimate the history of lineage diversification in *Labridae*. Because we subsampled our species dataset in the tip-dating analyses, we only used the full samples present in the node-dated phylogenies for all diversification rate estimates. For all diversification rate analyses, we removed all outgroups except *Centrogenys* as we were interested in testing whether there is a shift in diversification rates associated with *Labridae* and its immediate species-poor outgroup.

First, we used BAMM v 2.5.0 (*127*, *128*) to estimate diversification rates through time and associated shifts using a reversible-jump Markov chain Monte Carlo (MCMC) methodology. Input priors were generated on versions of the node-dated trees in R, which we forced to be ultrametric using commands in the ape package (*125*) using the R package BAMMTools (*129*). Because precise estimates of subfamily-level clade species diversity in Labridae are not available in Eschemeyer's Catalog nor are likely to be accurate given the rapid rate of species discovery and description in the wrasses and parrotfishes, we elected to input a global sampling fraction into the BAMM input file equal to 0.59, the proportion of labrids and *Centrogenys* sampled. We ran each BAMM chain for 5.0×10^7 generations and assessed for convergence of the posteriors and adequate effective sampled size values in R.

Next, we used TeSS-CoMET in R to calculate speciation, extinction, and diversification rates and associated shift posterior probabilities (*130*). We set the number of mass extinctions as 1, meaning that a mass extinction could occur once across the timescale of labrid evolution. This was intended to reflect the Grande Coupure (Eocene-Oligocene extinction event) and its effect on marine fish faunas (*22*). We ran different iterations changing the expected number of shifts from one to three following the recognition of potential major rapid radiation events in *Cirrhilabrinae* (*83*) and *Scarinae* (*131*), as well as the possibility that *Labridae* is a rapid radiation. We accounted for our sampling by inputting the proportion of species in *Labridae* and *Centrogenys* sampled in our tree (0.59) and set prior speciation (0.10) and extinction (0.02) parameters following the approximate estimates of reef-fish speciation and diversification rates found in a previous analysis of acanthomorph diversification (*65*), with an SD of 0.005. We also set the global survival probability to 0.90 following the observation that 90% or more marine animal species survived the Eocene-Oligocene extinction event (*29*, *132*, *133*) and replicated all analyses across the two different node-dated trees. We ran TeSS-CoMET for 1.0×10^7 generations with a 3.0×10^5 burn-in and minimum ESS > 200.

Historical biogeography and dispersal through time

Information on the geographic distribution of sampled species of *Labridae* and the time calibrated phylogeny was used to assess whether major shifts in the biogeography of labrids have occurred over their evolutionary history. To analyze labrid biogeography, we inputted the pruned node-dated trees (see "Comparative diversification rate estimates") and made a geographic distribution list for included species that we scored for eight areas (western Indian Ocean, central Indo-Pacific, eastern Indo-Pacific, temperate Australasia, central Pacific, eastern Pacific, western Atlantic, and eastern Atlantic/Mediterranean) following previous studies (*134*–*136*). We loaded these files into R for analysis using the package BioGeoBears (*137*).

After ensuring that the phylogeny was ultrametric and contained exclusively positive branch lengths following BioGeoBears requirements, we conducted historical biogeographic reconstructions using three different models: dispersal-extinction-cladogenesis, dispersal-vicariance–like, and a Bayesian model (BAYAREALIKE). We ran these models with and without the jump dispersal parameter j, resulting in six iterations. We then calculated log-likelihoods, Akaike information criterion (AIC) values, and corrected AIC values to select the best-fit model. The analyses using both node-dated trees (GTR and HKY) produced virtually identical AIC and log-likelihood values for the BAYAREALIKE and BAYAREALIKE+j models (weighted AIC values differed by ~1×10^{-4}), we chose the model with fewer parameters. We then reran a historical biogeographic reconstruction under the selected best-fit model (BAYAREALIKE) for biogeographic stochastic mapping (BSM) analysis, which estimates the number and type of biogeographic events occurring in a clade over time by producing simulated histories that explain the ancestral biogeographic

reconstruction found in the input model for a given phylogeny (*138*). We conducted BSMs with 100 as the maximum number of maps to try, 50 as the goal number, and 400 tries per branch. Next, we extracted and plotted the number of branch-wise (anagenetic) dispersal events through time for each discrete biogeographic region, as well as histograms displaying the number of counts for each biogeographic event: anagenetic dispersal, vicariance, narrow and subset sympatry, and founder events.

Comparison to the fossil record

We visually compared the diversification curves and lineage-through-time plots generated using our time-calibrated phylogenies to the labrid and acanthomorph fossils records. We downloaded all records for "*Labridae*" and "*Acanthomorphata*" (=*Acanthomorpha*) in the online Paleobiology Database. We then examined the downloaded datasets and removed obviously erroneous data points (for example, several occurrences included in the *Acanthomorpha* dataset were given Silurian age dates). We then plotted density curves for these occurrences datasets in R with an adjust sensitivity factor of 0.5.

Ancestral state reconstructions and disparity through time

Labridae is known for its exceptional morphological disparity, which includes numerous features thought to be key innovations that promoted their high species diversity (*47*, *52*, *53*, *66*, *69*, *131*, *139*). To reconstruct the evolution of these key innovations through time, we conducted discrete trait ancestral state reconstructions in the R package phytools using single-stochastic character mapping more than 1000 simulations for each of the six discrete traits cataloged by Burress and Wainwright (*52*) present in more than five wrasse species in our tree, as well as for the biting-suction trait recorded by Corn *et al.* (*67*), along our node-dated tree generated using the GTR model. To reconstruct the historical disparification of key continuous traits in Labridae, we used the R package geiger (*140*) to estimate disparity through time for 11 cranial skeletal and muscular traits and one postcranial trait (fin aspect ratio). Log-transformed data from Burress and Wainwright (*52*) were read into R, and traits found to be correlated with body size by Burress and Wainwright (*52*) were regressed against standard length so that residuals could be used for subsequent analysis. We fitted four models available in Geiger, Brownian Motion, OU, Early Burst, and White Noise, and compared them using AIC values. Next, we conducted node-height tests and plotted estimated disparity through time curves for each trait. Last, we used functions in phytools and geiger to plot traitgrams and conduct phylogenetic principal components analysis on the log-transformed continuous trait values (or residuals if they were found to correlate with body size).

Discrete trait-based diversification rates

Key innovations are defined as traits that facilitate the invasion of new ecologies by a clade and thus promote diversification (*72*). To establish whether any single discrete trait classically considered a key innovation in *Labridae* is associated with increased diversification across the clade, we estimated trait-based diversification rates in R using the BiSSE model (binary state dependent diversification rate analysis) implemented in the package diversitree (*141*) for each of the five binary traits along the node-dated phylogeny generated under the GTR model. We also assembled a dataset on labrid reef association and conducted the same BiSSE analysis protocol. We tested likelihood models where speciation rates were alternatively forced to be equal or allowed to differ and ran an MCMC for 10,000 generations on the best-fit model with sampling conducted every 100 generations. We checked for convergence of the posteriors following burning-in of 10% of generations in R and plotted histograms of estimated diversification rates associated with each state. For one nonbinary trait, biting mode, we conducted a multistate-dependent diversification rate analysis (MuSSE). We also ran this analysis using the R package diversitree after selecting the best-fit model from six different ones that differentially constrained transition, speciation, and extinction rates. MCMC specifications and assessment of convergence for the MuSSE analysis were the same as those for the BiSSE analyses.

To test the robustness of our inferences of trait-associated diversification rates to potential hidden states, we reran all BiSSE analyses using HiSSE models implemented in the R package hisse (*142*, *143*). We compared the fit of four models for trait-dependent diversification rates: (i) a null model in which turnover and extinction fraction did not differ between states, (ii) a BiSSE model in which turnover and extinction fraction were allowed to vary across states and no hidden states were allowed, (iii) a character-dependent HiSSE model where turnover and extinction fraction were allowed to vary across all states, and (iv) a character-independent HiSSE model in which turnover and extinction fraction were allowed to vary across hidden states but not known states. For the one trait type (biting versus suction versus both) that we initially analyzed using MuSSE, we ran three HiSSE analyses where the known character was variously treated as only biting versus all other states, only suction versus all other states, and both biting and suction versus all other states. For each of the discrete characters that we analyzed, we compared model fit using corrected AIC scores.

Continuous trait evolution and timing evolutionary optima

We used the R package bayou v 2.2.0 (*70*) to search for shifts in the adaptive optima of 12 continuous morphological traits extracted from Burress and Wainwright (*52*). We performed this step to evaluate in which moment during the radiation of labrids did these shifts occur. Bayou fits multi-optima OU models using a Bayesian reversible jump MCMC algorithm. We pruned the phylogeny to match morphological datasets (125 species). Following Burress and Wainwright (*52*), we phylogenetically corrected five size-corrected traits that strongly scale with standard length using the phyl.resid function implemented in phytools (*126*). The size-corrected traits were mouth gape, premaxillary protrusion, and *M. adductor mandibulae*, *M. sternohyoides*, and *M. levator posterior* masses. We then used the mean and SD of the empirical morphological distribution of each trait as starting values for theta (phenotypic optima) and set the prior for the maximum number of shifts as half of the number of branch lengths. We ran MCMC chains for 5 million generations for each trait, sampling every 1000 generations. We discarded the first 30% of generations as burn-in and assessed convergence by checking the tracer plot of the parameters and effect sample sizes. We considered only shifts with posterior probability greater than 30% and comprising more than two species to avoid spurious shifts.

Supplementary Materials

This PDF file includes:

Supplementary Text
Figs. S1 to S22
Tables S1 to S3
References

REFERENCES AND NOTES

1. J. T. Stroud, J. B. Losos, Ecological opportunity and adaptive radiation. *Annu. Rev. Ecol. Evol. Syst.* **47**, 507–532 (2016).
2. S. Gavrilets, J. B. Losos, Adaptive radiation: Contrasting theory with data. *Science* **323**, 732–737 (2009).
3. P. Hull, Life in the aftermath of mass extinctions. *Curr. Biol.* **25**, R941–R952 (2015).
4. D. M. Raup, J. J. Sepkoski, Mass extinctions in the marine fossil record. *Science* **215**, 1501–1503 (1982).
5. D. Schluter, *The Ecology of Adaptive Radiation* (OUP Oxford, 2000).
6. R. G. Gillespie, G. M. Bennett, L. De Meester, J. L. Feder, R. C. Fleischer, L. J. Harmon, A. P. Hendry, M. L. Knope, J. Mallet, C. Martin, C. E. Parent, A. H. Patton, K. S. Pfennig, D. Rubinoff, D. Schluter, O. Seehausen, K. L. Shaw, E. Stacy, M. Stervander, J. T. Stroud, C. Wagner, G. O. U. Wogan, Comparing adaptive radiations across space, time, and taxa. *J. Hered.* **111**, 1–20 (2020).
7. E. D. Jarvis, S. Mirarab, A. J. Aberer, B. Li, P. Houde, C. Li, S. Y. W. Ho, B. C. Faircloth, B. Nabholz, J. T. Howard, A. Suh, C. C. Weber, R. R. da Fonseca, J. Li, F. Zhang, H. Li, L. Zhou, N. Narula, L. Liu, G. Ganapathy, B. Boussau, M. S. Bayzid, V. Zavidovych, S. Subramanian, T. Gabaldón, S. Capella-Gutiérrez, J. Huerta-Cepas, B. Rekepalli, K. Munch, M. Schierup, B. Lindow, W. C. Warren, D. Ray, R. E. Green, M. W. Bruford, X. Zhan, A. Dixon, S. Li, N. Li, Y. Huang, E. P. Derryberry, M. F. Bertelsen, F. H. Sheldon, R. T. Brumfield, C. V. Mello, P. V. Lovell, M. Wirthlin, M. P. C. Schneider, F. Prosdocimi, J. A. Samaniego, A. M. V. Velazquez, A. Alfaro-Núñez, P. F. Campos, B. Petersen, T. Sicheritz-Ponten, A. Pas, T. Bailey, P. Scofield, M. Bunce, D. M. Lambert, Q. Zhou, P. Perelman, A. C. Driskell, B. Shapiro, Z. Xiong, Y. Zeng, S. Liu, Z. Li, B. Liu, K. Wu, J. Xiao, X. Yinqi, Q. Zheng, Y. Zhang, H. Yang, J. Wang, L. Smeds, F. E. Rheindt, M. Braun, J. Fjeldsa, L. Orlando, F. K. Barker, K. A. Jønsson, W. Johnson, K.-P. Koepfli, S. O'Brien, D. Haussler, O. A. Ryder, C. Rahbek, E. Willerslev, G. R. Graves, T. C. Glenn, J. McCormack, D. Burt, H. Ellegren, P. Alström, S. V. Edwards, A. Stamatakis, D. P. Mindell, J. Cracraft, E. L. Braun, T. Warnow, W. Jun, M. T. P. Gilbert, G. Zhang, Whole-genome analyses resolve early branches in the tree of life of modern birds. *Science* **346**, 1320–1331 (2014).
8. R. O. Prum, J. S. Berv, A. Dornburg, D. J. Field, J. P. Townsend, E. M. Lemmon, A. R. Lemmon, A comprehensive phylogeny of birds (Aves) using targeted next-generation DNA sequencing. *Nature* **526**, 569–573 (2015).
9. S. J. Hackett, R. T. Kimball, S. Reddy, R. C. K. Bowie, E. L. Braun, M. J. Braun, J. L. Chojnowski, W. A. Cox, K.-L. Han, J. Harshman, C. J. Huddleston, B. D. Marks, K. J. Miglia, W. S. Moore, F. H. Sheldon, D. W. Steadman, C. C. Witt, T. Yuri, A phylogenomic study of birds reveals their evolutionary history. *Science* **320**, 1763–1768 (2008).
10. S. L. Brusatte, J. K. O'Connor, E. D. Jarvis, The origin and diversification of birds. *Curr. Biol.* **25**, R888–R898 (2015).
11. D. J. Field, A. Bercovici, J. S. Berv, R. Dunn, D. E. Fastovsky, T. R. Lyson, V. Vajda, J. A. Gauthier, Early evolution of modern birds structured by global forest collapse at the end-Cretaceous mass extinction. *Curr. Biol.* **28**, 1825–1831.e2 (2018).
12. C. G. Klein, D. Pisani, D. J. Field, R. Lakin, M. A. Wills, N. R. Longrich, Evolution and dispersal of snakes across the Cretaceous-Paleogene mass extinction. *Nat. Commun.* **12**, 5335 (2021).
13. Y.-J. Feng, D. C. Blackburn, D. Liang, D. M. Hillis, D. B. Wake, D. C. Cannatella, P. Zhang, Phylogenomics reveals rapid, simultaneous diversification of three major clades of Gondwanan frogs at the Cretaceous–Paleogene boundary. *Proc. Natl. Acad. Sci.* **114**, E5864–E5870 (2017).
14. T. J. Near, A. Dornburg, R. I. Eytan, B. P. Keck, W. L. Smith, K. L. Kuhn, J. A. Moore, S. A. Price, F. T. Burbrink, M. Friedman, P. C. Wainwright, Phylogeny and tempo of diversification in the superradiation of spiny-rayed fishes. *Proc. Natl. Acad. Sci. U.S.A.* **110**, 12738–12743 (2013).
15. M. Friedman, Explosive morphological diversification of spiny-finned teleost fishes in the aftermath of the end-Cretaceous extinction. *Proc. Biol. Sci.* **277**, 1675–1683 (2010).
16. A. Ghezelayagh, R. C. Harrington, E. D. Burress, M. A. Campbell, J. C. Buckner, P. Chakrabarty, J. R. Glass, W. T. McCraney, P. J. Unmack, C. E. Thacker, M. E. Alfaro, S. T. Friedman, W. B. Ludt, P. F. Cowman, M. Friedman, S. A. Price, A. Dornburg, B. C. Faircloth, P. C. Wainwright, T. J. Near, Prolonged morphological expansion of spiny-rayed fishes following the end-Cretaceous. *Nat. Ecol. Evol.* **6**, 1211–1220 (2022).
17. M. E. Alfaro, B. C. Faircloth, R. C. Harrington, L. Sorenson, M. Friedman, C. E. Thacker, C. H. Oliveros, D. Černý, T. J. Near, Explosive diversification of marine fishes at the Cretaceous–Palaeogene boundary. *Nat. Ecol. Evol.* **2**, 688–696 (2018).
18. R. W. Meredith, J. E. Janečka, J. Gatesy, O. A. Ryder, C. A. Fisher, E. C. Teeling, A. Goodbla, E. Eizirik, T. L. L. Simão, T. Stadler, D. L. Rabosky, R. L. Honeycutt, J. J. Flynn, C. M. Ingram, C. Steiner, T. L. Williams, T. J. Robinson, A. Burk-Herrick, M. Westerman, N. A. Ayoub, M. S. Springer, W. J. Murphy, Impacts of the Cretaceous terrestrial revolution and KPg extinction on mammal diversification. *Science* **334**, 521–524 (2011).
19. S. Árez-Carretero, A. U. Tamuri, M. Battini, F. F. Nascimento, E. Carlisle, R. J. Asher, Z. Yang, P. C. J. Donoghue, M. dos Reis, A species-level timeline of mammal evolution integrating phylogenomic data. *Nature* **602**, 263–267 (2022).
20. N. M. Foley, V. C. Mason, A. J. Harris, K. R. Bredemeyer, J. Damas, H. A. Lewin, E. Eizirik, J. Gatesy, E. K. Karlsson, K. Lindblad-Toh, Zoonomia Consortium, M. S. Springer, W. J. Murphy, A genomic timescale for placental mammal evolution. *Science* **380**, eabl8189 (2023).
21. M. A. O'Leary, J. I. Bloch, J. J. Flynn, T. J. Gaudin, A. Giallombardo, N. P. Giannini, S. L. Goldberg, B. P. Kraatz, Z.-X. Luo, J. Meng, X. Ni, M. J. Novacek, F. A. Perini, Z. S. Randall, G. W. Rougier, E. J. Sargis, M. T. Silcox, N. B. Simmons, M. Spaulding, P. M. Velazco, M. Weksler, J. R. Wible, A. L. Cirranello, The placental mammal ancestor and the post-K-Pg radiation of placentals. *Science* **339**, 662–667 (2013).
22. D. Arcila, J. C. Tyler, Mass extinction in tetraodontiform fishes linked to the Palaeocene–Eocene thermal maximum. *Proc. Biol. Sci.* **284**, 20171771 (2017).
23. D. R. Prothero, The Late Eocene-Oligocene extinctions. *Annu. Rev. Earth Planet. Sci.* **22**, 145–165 (1994).
24. P. H. Kelley, T. A. Hansen, Recovery of the naticid gastropod predator-prey system from the Cretaceous-Tertiary and Eocene-Oligocene extinctions. *Geol. Soc. Lond. Spec. Publ.* **102**, 373–386 (1996).
25. D. de Vries, S. Heritage, M. R. Borths, H. M. Sallam, E. R. Seiffert, Widespread loss of mammalian lineage and dietary diversity in the early Oligocene of Afro-Arabia. *Commun. Biol.* **4**, 1172 (2021).
26. R. Weppe, F. L. Condamine, G. Guinot, J. Maugoust, M. J. Orliac, Drivers of the artiodactyl turnover in insular western Europe at the Eocene–Oligocene transition. *Proc. Natl. Acad. Sci. U.S.A.* **120**, e2309945120 (2023).
27. R. Zhang, V. A. Kravchinsky, L. Yue, Link between global cooling and mammalian transformation across the Eocene–Oligocene boundary in the continental interior of Asia. *Int. J. Earth Sci.* **101**, 2193–2200 (2012).
28. E. C. Sibert, R. D. Norris, New age of fishes initiated by the Cretaceous–Paleogene mass extinction. *Proc. Natl. Acad. Sci. U.S.A.* **112**, 8537–8542 (2015).
29. E. C. Sibert, M. E. Zill, E. T. Frigyik, R. D. Norris, No state change in pelagic fish production and biodiversity during the Eocene–Oligocene transition. *Nat. Geosci.* **13**, 238–242 (2020).
30. E. C. Sibert, P. M. Hull, R. D. Norris, Resilience of Pacific pelagic fish across the Cretaceous/Palaeogene mass extinction. *Nat. Geosci.* **7**, 667–670 (2014).
31. M. Bazzi, B. P. Kear, H. Blom, P. E. Ahlberg, N. E. Campione, Static dental disparity and morphological turnover in sharks across the End-Cretaceous mass extinction. *Curr. Biol.* **28**, 2607–2615.e3 (2018).
32. R. A. Belben, C. J. Underwood, Z. Johanson, R. J. Twitchett, Ecological impact of the end-Cretaceous extinction on lamniform sharks. *PLOS ONE* **12**, e0178294 (2017).
33. N. Santodomingo, W. Renema, K. G. Johnson, Understanding the murky history of the Coral Triangle: Miocene corals and reef habitats in East Kalimantan (Indonesia). *Coral Reefs* **35**, 765–781 (2016).
34. A. N. Campoy, M. M. Rivadeneira, C. E. Hernández, A. Meade, C. Venditti, Deep-sea origin and depth colonization associated with phenotypic innovations in scleractinian corals. *Nat. Commun.* **14**, 7458 (2023).
35. A. Lindner, S. D. Cairns, C. W. Cunningham, From offshore to onshore: Multiple origins of shallow-water corals from deep-sea ancestors. *PLOS ONE* **3**, e2429 (2008).
36. A. C. Siqueira, H. F. Yan, R. A. Morais, D. R. Bellwood, The evolution of fast-growing coral reef fishes. *Nature* **618**, 322–327 (2023).
37. K. M. Cantalice, J. Alvarado-Ortega, D. R. Bellwood, A. C. Siqueira, Rising from the ashes: The biogeographic origins of modern coral reef fishes. *Bioscience* **72**, 769–777 (2022).
38. M. Núñez-Flores, A. Solórzano, J. Avaria-Llautureo, D. Gomez-Uchida, P. J. López-González, Diversification dynamics of a common deep-sea octocoral family linked to the Paleocene-Eocene thermal maximum. *Mol. Phylogenet. Evol.* **190**, 107945 (2024).
39. L. Pellissier, F. Leprieur, V. Parravicini, P. F. Cowman, M. Kulbicki, G. Litsios, S. M. Olsen, M. S. Wisz, D. R. Bellwood, D. Mouillot, Quaternary coral reef refugia preserved fish diversity. *Science* **344**, 1016–1019 (2014).
40. A. C. Siqueira, P. Muruga, D. R. Bellwood, On the evolution of fish–coral interactions. *Ecol. Lett.* **26**, 1348–1358 (2023).
41. E. C. Sibert, L. D. Rubin, An early Miocene extinction in pelagic sharks. *Science* **372**, 1105–1107 (2021).
42. D. R. Bellwood, C. H. R. Goatley, O. Bellwood, The evolution of fishes and corals on reefs: Form, function and interdependence. *Biol. Rev.* **92**, 878–901 (2017).
43. J. D. DiBattista, M. E. Alfaro, L. Sorenson, J. H. Choat, J.-P. A. Hobbs, T. H. Sinclair-Taylor, L. A. Rocha, J. Chang, O. J. Luiz, P. F. Cowman, M. Friedman, M. L. Berumen, Ice ages and butterflyfishes: Phylogenomics elucidates the ecological and evolutionary history of reef fishes in an endemism hotspot. *Ecol. Evol.* **8**, 10989–11008 (2018).
44. P. F. Cowman, D. R. Bellwood, Coral reefs as drivers of cladogenesis: Expanding coral reefs, cryptic extinction events, and the development of biodiversity hotspots. *J. Evol. Biol.* **24**, 2543–2562 (2011).
45. W. Renema, D. R. Bellwood, J. C. Braga, K. Bromfield, R. Hall, K. G. Johnson, P. Lunt, C. P. Meyer, L. B. McMonagle, R. J. Morley, A. O'Dea, J. A. Todd, F. P. Wesselingh,

M. E. J. Wilson, J. M. Pandolfi, Hopping hotspots: Global shifts in marine biodiversity. *Science* **321**, 654–657 (2008).
46. S. R. Floeter, M. G. Bender, A. C. Siqueira, P. F. Cowman, Phylogenetic perspectives on reef fish functional traits. *Biol. Rev.* **93**, 131–151 (2018).
47. M. E. Alfaro, C. D. Brock, B. L. Banbury, P. C. Wainwright, Does evolutionary innovation in pharyngeal jaws lead to rapid lineage diversification in labrid fishes? *BMC Evol. Biol.* **9**, 255 (2009).
48. M. E. Alfaro, F. Santini, C. D. Brock, Do reefs drive diversification in marine teleosts? Evidence from the pufferfishes and their allies (Order Tetraodontiformes). *Evolution* **61**, 2104–2126 (2007).
49. D. R. Bellwood, S. Klanten, P. F. Cowman, M. S. Pratchett, N. Konow, L. Van HERWERDEN, Evolutionary history of the butterflyfishes (f: Chaetodontidae) and the rise of coral feeding fishes. *J. Evol. Biol.* **23**, 335–349 (2010).
50. J. L. Fessler, M. W. Westneat, Molecular phylogenetics of the butterflyfishes (Chaetodontidae): Taxonomy and biogeography of a global coral reef fish family. *Mol. Phylogenet. Evol.* **45**, 50–68 (2007).
51. J. J. Tavera, P. Arturo Acero, E. F. Balart, G. Bernardi, Molecular phylogeny of grunts (Teleostei, Haemulidae), with an emphasis on the ecology, evolution, and speciation history of New World species. *BMC Evol. Biol.* **12**, 57 (2012).
52. E. D. Burress, P. C. Wainwright, Adaptive radiation in labrid fishes: A central role for functional innovations during 65 My of relentless diversification. *Evolution* **73**, 346–359 (2019).
53. K. M. Evans, O. Larouche, S. M. Gartner, R. E. Faucher, S. G. Dee, M. W. Westneat, Beaks promote rapid morphological diversification along distinct evolutionary trajectories in labrid fishes (Eupercaria: Labridae). *Evolution* **77**, 2000–2014 (2023).
54. L. C. Hughes, C. M. Nash, W. T. White, M. W. Westneat, Concordance and discordance in the phylogenomics of the wrasses and parrotfishes (Teleostei: Labridae). *Syst. Biol.* **72**, 530–543 (2023).
55. B. S. Cramer, J. R. Toggweiler, J. D. Wright, M. E. Katz, K. G. Miller, Ocean overturning since the Late Cretaceous: Inferences from a new benthic foraminiferal isotope compilation. *Paleoceanogr. Paleoclimatol.* **24**, doi.org/10.1029/2008PA001683 (2009).
56. A. N. Meckler, P. F. Sexton, A. M. Piasecki, T. J. Leutert, J. Marquardt, M. Ziegler, T. Agterhuis, L. J. Lourens, J. W. B. Rae, J. Barnet, A. Tripati, S. M. Bernasconi, Cenozoic evolution of deep ocean temperature from clumped isotope thermometry. *Science* **377**, 86–90 (2022).
57. J. Zachos, M. Pagani, L. Sloan, E. Thomas, K. Billups, Trends, rhythms, and aberrations in global climate 65 Ma to present. *Science* **292**, 686–693 (2001).
58. M. Steinthorsdottir, H. K. Coxall, A. M. de Boer, M. Huber, N. Barbolini, C. D. Bradshaw, N. J. Burls, S. J. Feakins, E. Gasson, J. Henderiks, A. E. Holbourn, S. Kiel, M. J. Kohn, G. Knorr, W. M. Kürschner, C. H. Lear, D. Liebrand, D. J. Lunt, T. Mörs, P. N. Pearson, M. J. Pound, H. Stoll, C. A. E. Strömberg, The Miocene: The future of the past. *Paleoceanogr. Paleoclimatol.* **36**, e2020PA004037 (2021).
59. F. R. Bosellini, C. Perrin, Estimating Mediterranean Oligocene–Miocene sea-surface temperatures: An approach based on coral taxonomic richness. *Palaeogeogr. Palaeoclimatol. Palaeoecol.* **258**, 71–88 (2008).
60. K. G. Johnson, A. F. Budd, T. A. Stemann, Extinction selectivity and ecology of Neogene Caribbean Reef corals. *Paleobiology* **21**, 52–73 (1995).
61. M. W. Westneat, M. E. Alfaro, Phylogenetic relationships and evolutionary history of the reef fish family Labridae. *Mol. Phylogenet. Evol.* **36**, 370–390 (2005).
62. P. F. Cowman, D. R. Bellwood, L. van Herwerden, Dating the evolutionary origins of wrasse lineages (Labridae) and the rise of trophic novelty on coral reefs. *Mol. Phylogenet. Evol.* **52**, 621–631 (2009).
63. V. B. Baliga, C. J. Law, Cleaners among wrasses: Phylogenetics and evolutionary patterns of cleaning behavior within Labridae. *Mol. Phylogenet. Evol.* **94**, 424–435 (2016).
64. M. D. McGee, S. R. Borstein, J. I. Meier, D. A. Marques, S. Mwaiko, A. Taabu, M. A. Kishe, B. O'Meara, R. Bruggmann, L. Excoffier, O. Seehausen, The ecological and genomic basis of explosive adaptive radiation. *Nature* **586**, 75–79 (2020).
65. D. L. Rabosky, J. Chang, P. O. Title, P. F. Cowman, L. Sallan, M. Friedman, K. Kaschner, C. Garilao, T. J. Near, M. Coll, M. E. Alfaro, An inverse latitudinal gradient in speciation rate for marine fishes. *Nature* **559**, 392–395 (2018).
66. S. L. Sanderson, Versatility and specialization in labrid fishes: Ecomorphological implications. *Oecologia* **84**, 272–279 (1990).
67. K. A. Corn, S. T. Friedman, E. D. Burress, C. M. Martinez, O. Larouche, S. A. Price, P. C. Wainwright, The rise of biting during the Cenozoic fueled reef fish body shape diversification. *Proc. Natl. Acad. Sci. U.S.A.* **119**, e2119828119 (2022).
68. S. A. Price, R. Holzman, T. J. Near, P. C. Wainwright, Coral reefs promote the evolution of morphological diversity and ecological novelty in labrid fishes. *Ecol. Lett.* **14**, 462–469 (2011).
69. P. C. Wainwright, D. R. Bellwood, M. W. Westneat, J. R. Grubich, A. S. Hoey, A functional morphospace for the skull of labrid fishes: Patterns of diversity in a complex biomechanical system. *Biol. J. Linn. Soc.* **82**, 1–25 (2004).
70. J. C. Uyeda, L. J. Harmon, A novel Bayesian method for inferring and interpreting the dynamics of adaptive landscapes from phylogenetic comparative data. *Syst. Biol.* **63**, 902–918 (2014).
71. A. S. Roberts-Hugghis, C. M. Martinez, K. A. Corn, P. C. Wainwright, A classic key innovation constrains oral jaw functional diversification in fishes. *Evol. Lett.* **9**, 24–40 (2025).
72. A. H. Miller, J. T. Stroud, J. B. Losos, The ecology and evolution of key innovations. *Trends Ecol. Evol.* **38**, 122–131 (2023).
73. P. C. Wainwright, W. L. Smith, S. A. Price, K. L. Tang, J. S. Sparks, L. A. Ferry, K. L. Kuhn, R. I. Eytan, T. J. Near, The evolution of pharyngognathy: A phylogenetic and functional appraisal of the pharyngeal jaw key innovation in Labroid fishes and beyond. *Syst. Biol.* **61**, 1001–1027 (2012).
74. K. M. Evans, K. L. Williams, M. W. Westneat, Do coral reefs promote morphological diversification? Exploration of habitat effects on Labrid Pharyngeal jaw evolution in the era of big data. *Integr. Comp. Biol.* **59**, 696–704 (2019).
75. J. Hansen, M. Sato, G. Russell, P. Kharecha, Climate sensitivity, sea level and atmospheric carbon dioxide. *Philos. Trans. A Math. Phys. Eng. Sci.* **371**, 20120294 (2013).
76. W. Kiessling, Geologic and biologic controls on the evolution of reefs. *Annu. Rev. Ecol. Evol. Syst.* **40**, 173–192 (2009).
77. F. Leprieur, P. Descombes, T. Gaboriau, P. F. Cowman, V. Parravicini, M. Kulbicki, C. J. Melián, C. N. de Santana, C. Heine, D. Mouillot, D. R. Bellwood, L. Pellissier, Plate tectonics drive tropical reef biodiversity dynamics. *Nat. Commun.* **7**, 11461 (2016).
78. P. F. Cowman, Historical factors that have shaped the evolution of tropical reef fishes: A review of phylogenies, biogeography, and remaining questions. *Front. Genet.* **5**, 394 (2014).
79. S. Y. Tian, M. Yasuhara, F. L. Condamine, H.-H. M. Huang, A. G. S. Fernando, Y. M. Aguilar, H. Pandita, T. Irizuki, H. Iwatani, C. P. Shin, W. Renema, T. Kase, Cenozoic history of the tropical marine biodiversity hotspot. *Nature* **632**, 343–349 (2024).
80. A. Dornburg, J. Moore, J. M. Beaulieu, R. I. Eytan, T. J. Near, The impact of shifts in marine biodiversity hotspots on patterns of range evolution: Evidence from the Holocentridae (squirrelfishes and soldierfishes). *Evolution* **69**, 146–161 (2015).
81. M. Mathew, A. Makhankova, D. Menier, B. Sautter, C. Betzler, B. Pierson, The emergence of Miocene reefs in South China Sea and its resilient adaptability under varying eustatic, climatic and oceanographic conditions. *Sci. Rep.* **10**, 7141 (2020).
82. J. T. Streelman, M. Alfaro, M. W. Westneat, D. R. Bellwood, S. A. Karl, Evolutionary history of the parrotfishes: Biogeography, ecomorphology, and comparative diversity. *Evolution* **56**, 961–971 (2002).
83. Y.-K. Tea, X. Xu, J. D. DiBattista, N. Lo, P. F. Cowman, S. Y. W. Ho, Phylogenomic analysis of concatenated ultraconserved elements reveals the recent evolutionary radiation of the fairy Wrasses (Teleostei: Labridae: Cirrhilabrus). *Syst. Biol.* **71**, 1–12 (2022).
84. A. C. Siqueira, R. A. Morais, D. R. Bellwood, P. F. Cowman, Trophic innovations fuel reef fish diversification. *Nat. Commun.* **11**, 2669 (2020).
85. A. C. Siqueira, W. Kiessling, D. R. Bellwood, Fast-growing species shape the evolution of reef corals. *Nat. Commun.* **13**, 2426 (2022).
86. A. Dornburg, J. P. Townsend, M. Friedman, T. J. Near, Phylogenetic informativeness reconciles ray-finned fish molecular divergence times. *BMC Evol. Biol.* **14**, 169 (2014).
87. D. R. Bellwood, P. C. Wainwright, C. J. Fulton, A. S. Hoey, Functional versatility supports coral reef biodiversity. *Proc. Biol. Sci.* **273**, 101–107 (2006).
88. A. Bannikov, D. Bellwood, Zorzinilabrus furcatus, a new genus and species of labrid fish (Perciformes) from the Eocene of Bolca in northern Italy. *Studi e ricerche sui giacimenti terziari di Bolca* **18**, 5–14 (2017).
89. D. Bellwood, A new fossil fish Phyllopharyngodon longipinnis gen. et sp. nov. (family Labridae) from the Eocene, Monte Bolca, Italy. *Studi e Ricerche sui Giacimenti Terziari di Bolca* **6**, 149–160 (1990).
90. A. F. Bannikov, G. Carnevale, Bellwoodilabrus landinii n. gen., n. sp., a new genus and species of labrid fish (Teleostei, Perciformes) from the Eocene of Monte Bolca. *Geoderma* **32**, 201–220 (2010).
91. A. Bannikov, L. Sorbini, *Eocoris bloti*, a new genus and species of labrid fish (Perciformes, Labroidei) from the Eocene of Monte Bolca, Italy. *Studie Ricerche sui Giacimenti Terziari di Bolca* **6**, 133–148 (1990).
92. F. Leprieur, L. Pellissier, D. Mouillot, T. Gaboriau, Influence of historical changes in tropical reef habitat on the diversification of coral reef fishes. *Sci. Rep.* **11**, 20731 (2021).
93. K. de Queiroz, Toward an integrated system of clade names. *Syst. Biol.* **56**, 956–974 (2007).
94. K. de Queiroz, P. Cantino, *International Code of Phylogenetic Nomenclature (PhyloCode)* (CRC Press, 2020).
95. T. J. Near, C. E. Thacker, Phylogenetic classification of living and fossil ray-finned fishes (Actinopterygii). *Bull.- Peabody Mus. Nat. Hist* **65**, doi.org/10.3374/014.065.0101 (2024).
96. M. Thines, T. Aoki, P. W. Crous, K. D. Hyde, R. Lücking, E. Malosso, T. W. May, A. N. Miller, S. A. Redhead, A. M. Yurkov, D. L. Hawksworth, Setting scientific names at all taxonomic ranks in italics facilitates their quick recognition in scientific papers. *IMA Fungus* **11**, 25 (2020).
97. C. D. Brownstein, K. L. Zapfe, S. Lott, R. C. Harrington, A. Ghezelayagh, A. Dornburg, T. J. Near, Synergistic innovations enabled the radiation of anglerfishes in the deep open ocean. *Curr. Biol.* **34**, 2541–2550.e4 (2024).

98. Eschmeyer's Catalog of Fishes | California Academy of Sciences. https://calacademy.org/scientists/projects/eschmeyers-catalog-of-fishes.
99. R. C. Harrington, M. Kolmann, J. J. Day, B. C. Faircloth, M. Friedman, T. J. Near, Dispersal sweepstakes: Biotic interchange propelled air-breathing fishes across the globe. *J. Biogeogr.* **51**, 797–813 (2023).
100. P. F. Cowman, A. M. Quattrini, T. C. L. Bridge, G. J. Watkins-Colwell, N. Fadli, M. Grinblat, T. E. Roberts, C. S. McFadden, D. J. Miller, A. H. Baird, An enhanced target-enrichment bait set for Hexacorallia provides phylogenomic resolution of the staghorn corals (Acroporidae) and close relatives. *Mol. Phylogenet. Evol.* **153**, 106944 (2020).
101. F. Alda, W. B. Ludt, D. J. Elías, C. D. McMahan, P. Chakrabarty, Comparing ultraconserved elements and exons for phylogenomic analyses of middle American cichlids: When data agree to disagree. *Genome Biol. Evol.* **13**, evab161 (2021).
102. J. Stiller, S. Feng, A.-A. Chowdhury, I. Rivas-González, D. A. Duchêne, Q. Fang, Y. Deng, A. Kozlov, A. Stamatakis, S. Claramunt, J. M. T. Nguyen, S. Y. W. Ho, B. C. Faircloth, J. Haag, P. Houde, J. Cracraft, M. Balaban, U. Mai, G. Chen, R. Gao, C. Zhou, Y. Xie, Z. Huang, Z. Cao, Z. Yan, H. A. Ogilvie, L. Nakhleh, B. Lindow, B. Morel, J. Fjeldså, P. A. Hosner, R. R. da Fonseca, B. Petersen, J. A. Tobias, T. Székely, J. D. Kennedy, A. H. Reeve, A. Liker, M. Stervander, A. Antunes, D. T. Tietze, M. Bertelsen, F. Lei, C. Rahbek, G. R. Graves, M. H. Schierup, T. Warnow, E. L. Braun, M. T. P. Gilbert, E. D. Jarvis, S. Mirarab, G. Zhang, Complexity of avian evolution revealed by family-level genomes. *Nature* **629**, 851–860 (2024).
103. B. C. Faircloth, PHYLUCE is a software package for the analysis of conserved genomic loci. *Bioinformatics* **32**, 786–788 (2016).
104. S. Nurk, A. Bankevich, D. Antipov, A. A. Gurevich, A. Korobeynikov, A. Lapidus, A. D. Prjibelski, A. Pyshkin, A. Sirotkin, Y. Sirotkin, R. Stepanauskas, S. R. Clingenpeel, T. Woyke, J. S. McLean, R. Lasken, G. Tesler, M. A. Alekseyev, P. A. Pevzner, Assembling single-cell genomes and mini-metagenomes from chimeric MDA products. *J. Comput. Biol.* **20**, 714–737 (2013).
105. A. Bankevich, S. Nurk, D. Antipov, A. A. Gurevich, M. Dvorkin, A. S. Kulikov, V. M. Lesin, S. I. Nikolenko, S. Pham, A. D. Prjibelski, A. V. Pyshkin, A. V. Sirotkin, N. Vyahhi, G. Tesler, M. A. Alekseyev, P. A. Pevzner, SPAdes: A new genome assembly algorithm and its applications to single-cell sequencing. *J. Comput. Biol.* **19**, 455–477 (2012).
106. B. Q. Minh, H. A. Schmidt, O. Chernomor, D. Schrempf, M. D. Woodhams, A. von Haeseler, R. Lanfear, IQ-TREE 2: New models and efficient methods for phylogenetic inference in the genomic era. *Mol. Biol. Evol.* **37**, 1530–1534 (2020).
107. U. Mai, S. Mirarab, TreeShrink: Fast and accurate detection of outlier long branches in collections of phylogenetic trees. *BMC Genomics* **19**, 272 (2018).
108. R. Lanfear, P. B. Frandsen, A. M. Wright, T. Senfeld, B. Calcott, PartitionFinder 2: New methods for selecting partitioned models of evolution for molecular and morphological phylogenetic analyses. *Mol. Biol. Evol.* **34**, 772–773 (2017).
109. C. Zhang, M. Rabiee, E. Sayyari, S. Mirarab, ASTRAL-III: Polynomial time species tree reconstruction from partially resolved gene trees. *BMC Bioinformatics* **19**, 153 (2018).
110. S. Kalyaanamoorthy, B. Q. Minh, T. K. F. Wong, A. von Haeseler, L. S. Jermiin, ModelFinder: Fast model selection for accurate phylogenetic estimates. *Nat. Methods* **14**, 587–589 (2017).
111. B. Q. Minh, M. W. Hahn, R. Lanfear, New methods to calculate concordance factors for phylogenomic datasets. *Mol. Biol. Evol.* **37**, 2727–2733 (2020).
112. R. Bouckaert, J. Heled, D. Kühnert, T. Vaughan, C.-H. Wu, D. Xie, M. A. Suchard, A. Rambaut, A. J. Drummond, BEAST 2: A software platform for Bayesian evolutionary analysis. *PLoS Comput. Biol.* **10**, e1003537 (2014).
113. R. Bouckaert, T. G. Vaughan, J. Barido-Sottani, S. Duchêne, M. Fourment, A. Gavryushkina, J. Heled, G. Jones, D. Kühnert, N. D. Maio, M. Matschiner, F. K. Mendes, N. F. Müller, H. A. Ogilvie, L. du Plessis, A. Popinga, A. Rambaut, D. Rasmussen, I. Siveroni, M. A. Suchard, C.-H. Wu, D. Xie, C. Zhang, T. Stadler, A. J. Drummond, BEAST 2.5: An advanced software platform for Bayesian evolutionary analysis. *PLoS Comput. Biol.* **15**, e1006650 (2019).
114. A. Gavryushkina, D. Welch, T. Stadler, A. J. Drummond, Bayesian inference of sampled ancestor trees for epidemiology and fossil calibration. *PLoS Comput. Biol.* **10**, e1003919 (2014).
115. A. Gavryushkina, T. A. Heath, D. T. Ksepka, T. Stadler, D. Welch, A. J. Drummond, Bayesian total-evidence dating reveals the recent crown radiation of penguins. *Syst. Biol.* **66**, syw060 (2016).
116. C. D. Brownstein, Syngnathoid evolutionary history and the conundrum of fossil misplacement. *Integr. Org. Biol.* **5**, obad011 (2023).
117. M. Friedman, J. V. Andrews, H. Saad, S. El-Sayed, The Cretaceous–Paleogene transition in spiny-rayed fishes: Surveying "Patterson's Gap" in the acanthomorph skeletal record. *Geol. Belg.* **26**, doi: 10.20341/gb.2023.002 (2023).
118. T. J. Near, R. I. Eytan, A. Dornburg, K. L. Kuhn, J. A. Moore, M. P. Davis, P. C. Wainwright, M. Friedman, W. L. Smith, Resolution of ray-finned fish phylogeny and timing of diversification. *Proc. Natl. Acad. Sci. U.S.A.* **109**, 13698–13703 (2012).
119. L. C. Hughes, G. Ortí, Y. Huang, Y. Sun, C. C. Baldwin, A. W. Thompson, D. Arcila, R. Betancur-R, C. Li, L. Becker, N. Bellora, X. Zhao, X. Li, M. Wang, C. Fang, B. Xie, Z. Zhou, H. Huang, S. Chen, B. Venkatesh, Q. Shi, Comprehensive phylogeny of ray-finned fishes (Actinopterygii) based on transcriptomic and genomic data. *Proc. Natl. Acad. Sci. U.S.A.* **115**, 6249–6254 (2018).
120. R. A. Close, Z. Johanson, J. C. Tyler, R. C. Harrington, M. Friedman, Mosaicism in a new Eocene pufferfish highlights rapid morphological innovation near the origin of crown tetraodontiforms. *Palaeontology* **59**, 499–514 (2016).
121. A. Rambaut, A. J. Drummond, D. Xie, G. Baele, M. A. Suchard, Posterior summarization in Bayesian phylogenetics using Tracer 1.7. *Syst. Biol.* **67**, 901–904 (2018).
122. R. C. M. Warnock, Z. Yang, P. C. J. Donoghue, Exploring uncertainty in the calibration of the molecular clock. *Biol. Lett.* **8**, 156–159 (2011).
123. G. E. Budd, R. P. Mann, Two notorious nodes: A critical examination of relaxed molecular clock age estimates of the bilaterian animals and placental mammals. *Syst. Biol.* **73**, 223–234 (2023).
124. N. Mongiardino Koch, J. R. Thompson, A. S. Hiley, M. F. McCowin, A. F. Armstrong, S. E. Coppard, F. Aguilera, O. Bronstein, A. Kroh, R. Mooi, G. W. Rouse, Phylogenomic analyses of echinoid diversification prompt a re-evaluation of their fossil record. *eLife* **11**, e72460 (2022).
125. E. Paradis, J. Claude, K. Strimmer, APE: Analyses of phylogenetics and evolution in R language. *Bioinformatics* **20**, 289–290 (2004).
126. L. J. Revell, phytools: An R package for phylogenetic comparative biology (and other things). *Methods Ecol. Evol.* **3**, 217–223 (2012).
127. D. L. Rabosky, Automatic detection of key innovations, rate shifts, and diversity-dependence on phylogenetic trees. *PLOS ONE* **9**, e89543 (2014).
128. D. L. Rabosky, F. Santini, J. Eastman, S. A. Smith, B. Sidlauskas, J. Chang, M. E. Alfaro, Rates of speciation and morphological evolution are correlated across the largest vertebrate radiation. *Nat. Commun.* **4**, 1958 (2013).
129. D. L. Rabosky, M. Grundler, C. Anderson, P. Title, J. J. Shi, J. W. Brown, H. Huang, J. G. Larson, BAMMtools: An R package for the analysis of evolutionary dynamics on phylogenetic trees. *Methods Ecol. Evol.* **5**, 701–707 (2014).
130. S. Höhna, M. R. May, B. R. Moore, TESS: An R package for efficiently simulating phylogenetic trees and performing Bayesian inference of lineage diversification rates. *Bioinformatics* **32**, 789–791 (2016).
131. E. Kazancıoğlu, T. J. Near, R. Hanel, P. C. Wainwright, Influence of sexual selection and feeding functional morphology on diversification rate of parrotfishes (Scaridae). *Proc. Biol. Sci.* **276**, 3439–3446 (2009).
132. R. A. Rohde, R. A. Muller, Cycles in fossil diversity. *Nature* **434**, 208–210 (2005).
133. S. M. Stanley, Estimates of the magnitudes of major marine mass extinctions in earth history. *Proc. Natl. Acad. Sci. U.S.A.* **113**, E6325–E6334 (2016).
134. A. Santaquiteria, A. C. Siqueira, E. Duarte-Ribeiro, G. Carnevale, W. T. White, J. J. Pogonoski, C. C. Baldwin, G. Ortí, D. Arcila, B.-R. Ricardo, Phylogenomics and historical biogeography of seahorses, dragonets, goatfishes, and allies (Teleostei: Syngnatharia): Assessing factors driving uncertainty in biogeographic inferences. *Syst. Biol.* **70**, 1145–1162 (2021).
135. M. D. Spalding, H. E. Fox, G. R. Allen, N. Davidson, Z. A. Ferdana, C. Finlayson, B. S. Halpern, M. A. Jorge, A. Lombana, S. A. Lourie, K. D. Martin, E. McManus, J. Molnar, C. A. Recchia, J. Robertson, Marine ecoregions of the world: A bioregionalization of coastal and shelf areas. *Bioscience* **57**, 573–583 (2007).
136. M. Kulbicki, V. Parravicini, D. R. Bellwood, E. Arias-Gonzàlez, P. Chabanet, S. R. Floeter, A. Friedlander, J. McPherson, R. E. Myers, L. Vigliola, D. Mouillot, Global biogeography of reef fishes: A hierarchical quantitative delineation of regions. *PLOS ONE* **8**, e81847 (2013).
137. N. J. Matzke, Probabilistic historical biogeography: New models for founder-event speciation, imperfect detection, and fossils allow improved accuracy and model-testing. *Front. Biogeogr.* **5**, doi.org/10.21425/F5FBG19694 (2013).
138. J. Dupin, N. J. Matzke, T. Särkinen, S. Knapp, R. G. Olmstead, L. Bohs, S. D. Smith, Bayesian estimation of the global biogeographical history of the Solanaceae. *J. Biogeogr.* **44**, 887–899 (2017).
139. K. F. Liem, S. L. Sanderson, The pharyngeal jaw apparatus of labrid fishes: A functional morphological perspective. *J. Morphol.* **187**, 143–158 (1986).
140. L. J. Harmon, J. T. Weir, C. D. Brock, R. E. Glor, W. Challenger, GEIGER: Investigating evolutionary radiations. *Bioinformatics* **24**, 129–131 (2008).
141. R. G. FitzJohn, Diversitree: Comparative phylogenetic analyses of diversification in R: *Diversitree*. *Methods Ecol. Evol.* **3**, 1084–1092 (2012).
142. J. Beaulieu, B. O'Meara, D. Caetano, J. Boyko, T. Vasconcelos, hisse: Hidden State Speciation and Extinction, version 2.1.11 (2023); https://cran.r-project.org/web/packages/hisse/index.html.
143. J. M. Beaulieu, B. C. O'Meara, Detecting hidden diversification shifts in models of trait-dependent speciation and extinction. *Syst. Biol.* **65**, 583–601 (2016).
144. G. Carnevale, S. J. Godfrey, T. W. Pietsch, Stargazer (Teleostei, Uranoscopidae) cranial remains from the Miocene Calvert Cliffs, Maryland, U.S.A. (St. Marys Formation, Chesapeake Group). *J. Vertebr. Paleontol.* **31**, 1200–1209 (2011).
145. G. Carnevale, S. J. Godfrey, Miocene bony fishes of the Calvert, Choptank, St. Marys and Eastover Formations, Chesapeake Group, Maryland and Virginia. *Smithsonian Contributions to Paleobiology* **100**, 161–212 (2018).

146. D. R. Bellwood, O. Schultz, A. C. Siqueira, P. F. Cowman, A review of the fossil record of the Labridae. *Ann. Naturhist. Mus. Wien, Serie A* **121**, 125–194 (2019).
147. M. Friedman, G. Carnevale, The Bolca Lagerstätten: hallow marine life in the Eocene. *J. Geol. Soc. London* **175**, 569–579 (2018).
148. O. Schultz, D. Bellwood, Trigonodon oweni and Asima jugleri are different parts of the same species Trigonodon jugleri, a Chiseltooth Wrasse from the Lower and Middle Miocene in Central Europe (Osteichthyes, Labridae, Trigonodontinae). *Ann. Naturhist. Mus. Wien* **105**, 287–305 (2004).
149. F. M. Gradstein, J. G. Ogg, M. Schmitz, G. Ogg, *The Geologic Time Scale 2020* (Elsevier Science, 2020), 53, 497, 504.
150. D. Bellwood, O. Schultz, A review of the fossil record of the parrotfishes (Labroidei: Scaridae) with a description of a New Calotomus species from the Middle Miocene (Badenian) of Austria. *Ann. Naturhist. Mus. Wien.* **92**, 55–71 (1991).
151. G. Carnevale, Middle Miocene wrasses (Teleostei, Labridae) from St. Margarethen (Burgenland, Austria) [121–159]. *Palaeontogr. Abt. A* **304**, 124–160 (2015).
152. J. Hohenegger, S. Ćorić, M. Wagreich, Timing of the Middle Miocene Badenian Stage of the Central Paratethys. *Geol. Carpath.* **65**, 55–66 (2014).
153. A. F. Bannikov, D. R. Bellwood, A new genus and species of labrid fish (Perciformes) from the Eocene of Bolca in northern Italy. *Studi e ricerche sui giacimenti terziari di Bolca* **16**, 5–16 (2015).
154. A. F. Bannikov, R. Zorzin, *Paralabrus rossiae*, a new genus and species of putative labroid fish (Perciformes) from the Eocene of Bolca in northern Italy. *Studi e ricerche sui giacimenti terziari di Bolca* **16**, 39–47 (2019).
155. B. C. Russell, Revision of the labrid fish genus Pseudolabrus and allied genera. *Records of the Australian Museum, Supplement* **9**, 1–72 (1988).
156. M. W. Westneat, Phylogenetic relationships of the Tribe Cheilinini (Labridae: Perciformes). *Bull. Marine Sci.* **52**, 351–394 (1993).
157. M. F. Gomon, Relationships of fishes of the labrid tribe Hypsigenyini. *Bull. Marine Sci.* **60**, 789–871 (1997).
158. Y.-K. Tea, G. R. Allen, C. H. R. Goatley, A. C. Gill, B. W. Frable, Redescription of Conniella apterygia Allen and its reassignment in the genus Cirrhilabrus Temminck and Schlegel (Teleostei: Labridae), with comments on cirrhilabrin pelvic morphology. *Zootaxa* **5061**, 493–509 (2021).
159. R. Fricke, W. N. Eschmeyer, R. V. D. Laan, Eschmeyer's Catalog of Fishes: Genera, Species, References., Electronic Version. http://researcharchive.calacademy.org/research/ichthyology/catalog/fishcatmain.asp.

Acknowledgments: We thank members of the Near and Muñoz laboratories for discussions regarding this paper. J.T. collected specimens under Colombian permit number 20182200001023 (Colombian National Natural Parks) and ANLA resolution 1070 28 (August 2015). We also thank Y. K. Tea for providing several cirrhilabrine tissue samples and for discussions related to this paper. We thank G. J. Watkins-Colwell of the Yale Peabody Museum for assisting with DNA sample curation and transfer; J. Klunk from Arbor Bioscience for assistance with target capture sequencing; J. Hung for assistance with DNA extractions and quantification; S. Klanten, R. Robertson, and L. Liggins for providing several parrotfish and wrasse tissue samples; and collections staff at the Australian Museum, Museum Victoria, Te Papa Museum for assisting with tissue loans. **Funding:** C.D.B. is supported by the Yale Training Program in Genetics. T.J.N. is supported by the Bigham Oceanographic Fund from the Yale Peabody Museum and the National Science Foundation (grant no. DEB-2508461). Targeted capture sequencing was supported by the Australian Research Council through the ARC Discovery Early Career Researcher Award to P.F.C. (DE170100516), with salary support to P.F.C. from the ARC Centre of Excellence for Coral Reef Studies (CE140100020). **Authorship contributions:** Conceptualization: J.H.C., L.A.R., P.C.W., M.M.M., C.D.B., P.F.C., D.R.B., and T.J.N. Resources: J.T., J.H.C., L.A.R., P.C.W., M.M.M., C.D.B., P.F.C., D.R.B., and T.J.N. Methodology: J.T., M.M.M., C.D.B., P.F.C., L.R.V.A., T.J.N., and R.C.H. Funding acquisition: C.D.B., P.F.C., D.R.B., and T.J.N. Investigation: J.T., J.H.C., C.D.B., P.F.C., E.D.B., T.J.N., and R.C.H. Visualization: J.H.C., L.A.R., C.D.B., L.R.V.A., and T.J.N. Validation: J.H.C., L.A.R., C.D.B., P.F.C., L.R.V.A., and T.J.N. Software: C.D.B., L.R.V.A., and P.F.C. Supervision: M.M.M., P.F.C., T.J.N., and C.D.B. Writing—original draft: C.D.B. and T.J.N. Writing—review and editing: C.D.B., R.C.H., L.R.V.A., D.R.B., J.H.C., L.A.R., P.C.W., J.T., E.D.B., M.M.M., P.F.C., and T.J.N. Data curation: C.D.B., P.F.C., E.D.B., T.J.N., and R.C.H. Formal analysis: C.D.B., P.F.C., L.R.V.A., T.J.N., and R.C.H. Project administration: C.D.B., P.F.C., and T.J.N. **Competing interests:** The authors declare that they have no competing interests. **Data and materials availability:** All data needed to evaluate the conclusions in the paper are present in the paper and/or the Supplementary Materials, including on the Dryad repository associated with this article (10.5061/dryad.f7m0cfz5x). Sequence data are available on the NCBI repository Genbank: BioProject PRJNA1114898.

Submitted 13 November 2024
Accepted 28 March 2025
Published 7 May 2025
10.1126/sciadv.adu6149